On Solutions to a Nonlinear Elliptic Equation

California State Polytechnic University, Pomona

and

Loyola Marymount University

Department of Mathematics Technical Report

Michael Grigsby[*], Cathy Ho[†], Adriana Melgoza[‡], Hernan Oscco [§], Michelle Craddock[¶], Maria Mercedes Franco [‖]

Applied Mathematical Sciences Summer Institute
Department of Mathematics & Statistics
California State Polytechnic University Pomona
3801 W. Temple Ave.
Pomona, CA 91768

August 2006

[*]California State Polytechnic University, Pomona
[†]Boston University
[‡]Loyola Marymount University
[§]California State Polytechnic University, Pomona
[¶]University of Mississippi
[‖]Queensborough Community College

1 Abstract

Our research focuses on the nonlinear, elliptic partial differential equation

$$-\Delta u = |u|^{p-1}u + \lambda u \text{ in } \quad , \quad u \not\equiv 0 \text{ in } \quad , \quad u = 0 \text{ on } \partial \quad , \tag{1}$$

where is a bounded domain in $\mathbb{R}^n$, $n \geq 3$, and $p = \frac{n+2}{n-2}$ is Sobolev's critical exponent. The origin of (1) can be traced back to physics and geometry problems, such as Yamabe-type problems. (1) has been exhaustively studied for $n \geq 4$. Of the many open questions for $n = 3$, we address the existence of radially symmetric solutions when $= B(0, R)$, in which case (1) reduces to

$$-u'' - \frac{2}{r}u' = u^5 + \lambda u, \quad 0 < r < R, \quad u'(0) = 0, \quad u(R) = 0 \tag{2}$$

(notice the singularity at the origin). Building upon [10], we use numerical methods to study (2), thus posing the conjecture:

> Let $\lambda_j = (\frac{j\pi}{R})^2, j = 1, 2, \ldots$ be the eigenvalues for the linearized problem associated with (2) and $\lambda_j^* = (1 - \frac{1}{2j})^2\lambda_j$. For every $\lambda \in (\lambda_j^*, \lambda_j)$, there is a solution pair $\{u_\lambda, -u_\lambda\}$. Moreover, $\|u_\lambda\|_\infty \to 0$ as $\lambda \to \lambda_j^-$ and $\|u_\lambda\|_\infty \to \infty$ as $\lambda \to (\lambda_j^*)^+$.

Our conjecture and its supporting evidence agree with the results of [2] and significantly add to those of [4].

2 Background

2.1 Motivation

Let be a bounded domain in $\mathbb{R}^n$, with $n \geq 3$. Consider the nonlinear elliptic boundary value problem:

$$\begin{aligned} -\Delta u = |u|^{p-1}u + f(x, u) \quad &\text{in} \quad , \\ u \not\equiv 0 \quad &\text{in} \quad , \\ u = 0 \quad &\text{on } \partial \quad , \end{aligned} \tag{3}$$

where $p = \frac{(n+2)}{(n-2)}$, $f(x, 0) = 0$, and $f(x, u)$ is a lower order perturbation of u^p, that is, $\lim_{u\to\infty} \frac{f(x,u)}{u^p} = 0$. The solutions of (3) are critical values of the functional

$$\Phi(u) = \frac{1}{2}\int\left(|\nabla u|^2 - \frac{1}{p+1}\int |u|^{p+1} - \int\right(F(x, u),$$

where $F(x, u) = \int_0^u f(x, t)dt$. This problem offers serious difficulties when trying to find critical points by standard variational methods (A.2).

The existence of positive solutions to (3) has been largely studied. The interest in positive solutions derives from variational problems in geometry (the best example is Yamabe's problem, A.8) and physics (A.4).

2.2 Known Results

In a first attempt to narrow down the PDE (3), we assume that $f(x,u) = \lambda u$, $\lambda \in \mathbb{R}$. Thus, problem (3) reduces to

$$\begin{aligned} -\Delta u &= |u|^{p-1}u + \lambda u \quad \text{in} \quad , \\ u &\not\equiv 0 \qquad\quad \text{in} \quad , \\ u &= 0 \qquad\quad \text{on } \partial \quad . \end{aligned} \tag{4}$$

Recall that $p = \frac{n+2}{n-2}$ and is a bounded domain in $\mathbb{R}^n$. Let λ_j, $j \in \mathbb{N}$, be the eigenvalues of the linearized problem associated with (4). This linear equation is known as the Dirichlet's problem for the operator $-\Delta$. It is known that:

1. If $\lambda < 0$ and is a ball in $\mathbb{R}^n$, then (4) has no solution [15].

2. If $\lambda > \lambda_1$, then there are no positive solutions of (4). (This is a well-known fact. For a proof, see [10].)

3. If is a ball in $\mathbb{R}^n$, then every positive solution of (4) is radially symmetric [12].

4. If $n = 3$ and is the unit ball, then (4) has a positive solution if and only if $\lambda \in (\frac{1}{4}\lambda_1, \lambda_1)$. Moreover, if $\lambda \leq \frac{1}{4}\lambda_1$ then there are no radially symmetric solutions of (4) [2].

5. If $\lambda \in (\tilde{\lambda_j}, \lambda_j)$, for some $\tilde{\lambda_j}$ that depends on the domain and the dimension, then problem (4) has at least m_j pairs of solutions

$$\{u_k(\lambda), -u_k(\lambda)\}, \qquad k = 1, 2, \ldots, m_j$$

   where m_j is the multiplicity of λ_j [4].

6. If is star-shaped, then there are no positive solutions of (4) for $\lambda \leq 0$ [15].

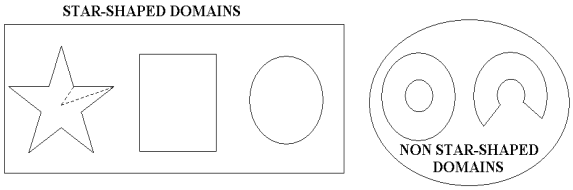

7. If $n \geq 4$, then for all $\lambda \in (0, \lambda_1)$ there exists a positive solution of (4) [2].

8. If $n \geq 4$, then for all $\lambda > 0$ problem (4) has infinitely many solutions, not necessarily symmetric, that change sign [9].

9. If $n = 4$, 5 or 6, then there exist a constant $\lambda^* > 0$ such that for all $\lambda < \lambda^*$ problem (4) does not have radially symmetric solutions that change sign [1].

10. If $n \geq 7$, then for all $\lambda > 0$ there exist infinitely many solutions of (4) that are radially symmetric and change sign [5].

3 Our Problem

PDE (3) was narrowed to (4). We are now going to focus our research on problem (4) when $n = 3$, $= B(0, R)$, and $R > 0$. Thus, we study the (highly) nonlinear, elliptic partial differential equation

$$\begin{aligned} -\Delta u &= u^5 + \lambda u \text{ in } B \\ u &\not\equiv 0 \text{ in } B \\ u &= 0 \text{ on } \partial B. \end{aligned} \tag{5}$$

3.1 Why is it a problem?

Despite its simple form, (5) is particularly difficult to study when $n = 3$ because of its high nonlinearity compared to the higher dimensional versions ($n \geq 4$). Let's step back to problem (4) which is posed for general n. When $n = 3$, $p = 5$, but when $n = 4$, $p = 3$. As the dimension increases, the nonlinear term of (4), $|u|^{p-1}u$, becomes less and less nonlinear because $\lim_{n\to\infty} p = \lim_{n\to\infty} \frac{n+2}{n-2} = 1$. Thus, the term $|u|^{p-1}u$ tends to u.

Notice how in higher dimensions ($n \geq 4$), as seen in section 2.2, there is an abundance of results addressing existence of all types of solutions: positive as well as sign-changing solutions and solutions with and without radial symmetry.

3.2 What needs to be studied?

Based on the known results of section 2.2, we have a foundation on which to build our research.

The top graph in figure 1 shows what is already known for problem (5) when $R = 1$, that is, when our domain is the unit ball $B(0, 1) \subset \mathbb{R}^3$. The eigenvalues are known to have the form $\lambda_j = (j\pi)^2$, $j \in \mathbb{N}$. It is known that radially symmetric, positive solutions exist exclusively in the λ_1 interval $(\frac{\lambda_1}{4}, \lambda_1)$ (items 2.1.3 and 2.1.4). It is also known that solutions exist in the λ_j intervals $(\tilde{\lambda_1}, \lambda_1)$, $(\tilde{\lambda_2}, \lambda_2)$, $\ldots, (\tilde{\lambda_j}, \lambda_j)$ (item 2.1. 5). Combining the above results, it follows that the solutions in the λ_j intervals for $j \geq 2$ *must change sign.* Note that these results do not say whether these sign-changing solutions are radially symmetric. Also note that the $(\tilde{\lambda_j}, \lambda_j)$ intervals are not drawn to scale so as to convey a better visualization; in reality, they are much narrower, specifically, $\lambda_j - \tilde{\lambda_j} = 0.1380$ [4]. Finally, the graph incorporates the fact that no solution exists for $\lambda < 0$ (item 2.1.1).

The bottom graph of figure 1 shows what has already been studied in [10] concerning the unit ball. Based on the study of the first two λ_j intervals, the following conjecture was posed in [10]:

Conjecture 1. *If $\lambda \in (\lambda_j^*, \lambda_j)$, where $(\lambda_j^*)^{1/2} - (\lambda_j)^{1/2} = \frac{\pi}{2}$, then PDE (5) with $R = 1$ has a pair of radially symmetric solutions $\{u_\lambda, -u_\lambda\}$. Moreover, $\|u_\lambda\|_\infty \to 0$ as $\lambda \to \lambda_j^-$ and $\|u_\lambda\|_\infty \to \infty$ as $\lambda \to (\lambda_j^*)^+$.*

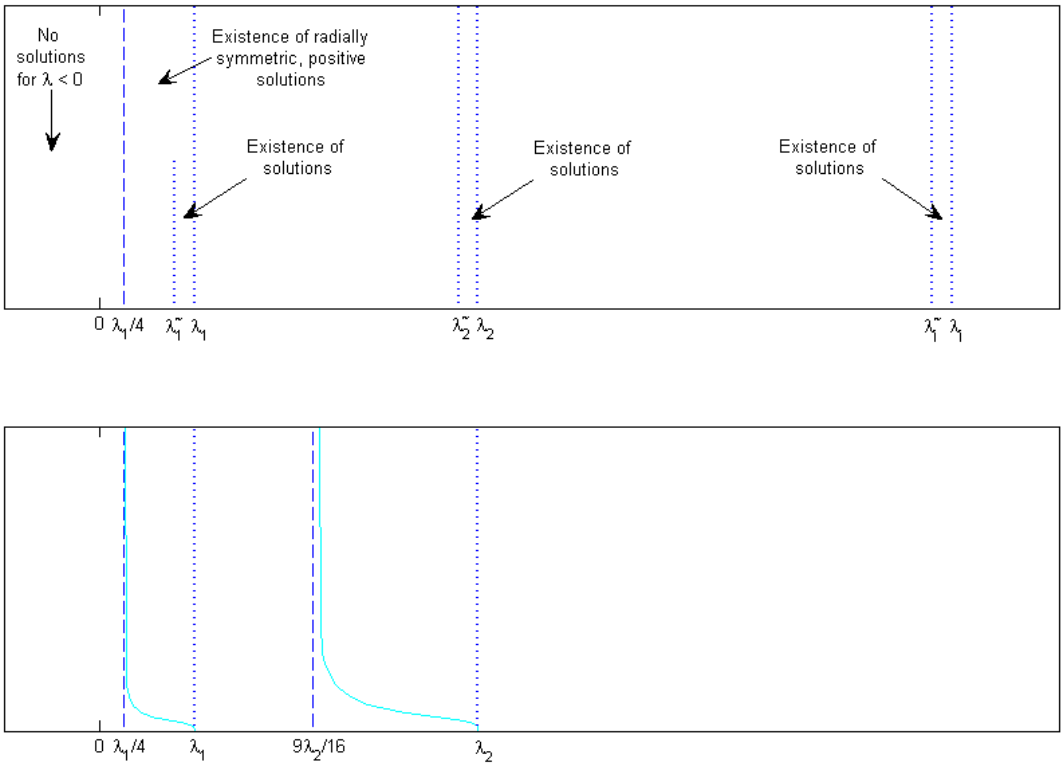

Figure 1: Top: Graphical representation of items 1, 3, 4, and 5 from section 2.2, when $= B(0,1) \subset \mathbb{R}$. Bottom: Results from [10].

We focus on exploring the existence and qualitative behavior of radially symmetric solutions of (5). First, we study to see if our research supports the conjecture (from [10]) for $R = 1$. Then we try other domains besides the unit ball. We test to see how solutions behave qualitatively in different λ_j intervals (λ_j^*, λ_j), $j \in \mathbb{N}$, for $R > 0$. We also want to estimate values for the left bound, λ_j^*, of the different λ_j intervals and hopefully prove that asymptotes exist at those left bounds. In addition, we want to solve for a solution to our problem (5).

3.3 Reducing Our PDE to an ODE

Assuming that the solutions of (5) are radially symmetric, we get the following ordinary differential equation:

$$\begin{aligned} -u'' - \frac{2}{r}u' &= u^5 + \lambda u, \quad 0 < r < R, \\ u'(0) &= 0 \\ u(R) &= 0 \end{aligned} \tag{6}$$

Due to the radial symmetry, the solutions will only depend on r, thus,

$$
\begin{aligned}
-\Delta u &= -u_{rr} - \frac{2}{r}u_r - \frac{1}{r^2}u_{\theta\theta} - \frac{1}{r^2 sin^2\theta}u_{\phi\phi} - \frac{cos\theta}{r^2 sin\theta}u_\phi \\
&\quad \text{(Laplacian in spherical coordinates)} \\
&= -u_{rr} - \frac{2}{r}u_r \\
&\quad \text{(other partial derivatives vanish, since } u \text{ does not depend on } \theta \text{ nor } \phi) \\
&= -u'' - \frac{2}{r}u' \\
&\quad \text{(no need for partial derivative notation since } u \text{ is a function of a single} \\
&\quad \text{variable, } r).
\end{aligned}
$$

This justifies the left hand side of the ODE (6) above.

4 Numerical Methods

The boundary value problem (BVP) (6) is much too difficult to solve using analytical techniques, therefore numerical techniques are used instead. Particularly we use the **nonlinear shooting method**. In general, linear and nonlinear shooting methods are used to solve BVPs.

The linear shooting method expresses solutions to linear BVPs as a linear combination of solutions to the individual initial value problems (IVPs), one for each boundary condition. The solution to a nonlinear problem cannot be expressed as a linear combination of solutions to the IVPs. Instead we use the nonlinear shooting method.

4.1 The Nonlinear Shooting Method - Overview

The nonlinear shooting method approximates solutions to nonlinear BVPs using solutions to a sequence of initial value problems (IVPs) involving some parameter, such as the value of the solution at a specified point or the derivative of the solution at a specified point [3]. The value of this parameter is adjusted until the solution satisfies the boundary conditions.

For our problem, we start by fixing the value for λ. Then we make an initial guess to the value of the solution at $r = 0$, because only the derivative of the solution at this point is known. Since solutions always come in pairs, (that is, if u is a solution, then so is -u) then without loss of generality we choose a nonnegative initial guess. Call this guess a_0. Using $u(0) = a_0$ we pose the following IVP,

$$
\begin{aligned}
-u'' - \frac{2}{r}u' &= \lambda u + u^5 \\
u'(0) &= 0 \\
u(0) &= a_0
\end{aligned}
\tag{7}
$$

where $a_0 > 0$. Our method then "shoots" the solution that we denote by $u_\lambda(\cdot, a_0)$, to the IVP (7). If $u_\lambda(R, a_0) = 0$, then this is the solution to our BVP (6). However, if $u_\lambda(R, a_0) \neq 0$,

then a new guess is used for $u(0)$ and we pose another IVP using this guess,

$$\begin{aligned} -u'' - \frac{2}{r}u' &= \lambda u + u^5 \\ u'(0) &= 0 \\ u(0) &= a_1 \end{aligned} \tag{8}$$

where $a_1 > 0$. If the solution to (8), denoted by $u_\lambda(\cdot, a_1)$, satisfies the boundary condition at $r = R$, then $u_\lambda(\cdot, a_1)$ is the solution to our BVP (6). Likewise if $u_\lambda(R, a_1) \neq 0$, then another guess, say $a_2 > 0$, is used for $u(0)$. In this manner, a sequence of IVPs and their corresponding solutions are obtained until a solution that satisfies the BVP (6) is found.

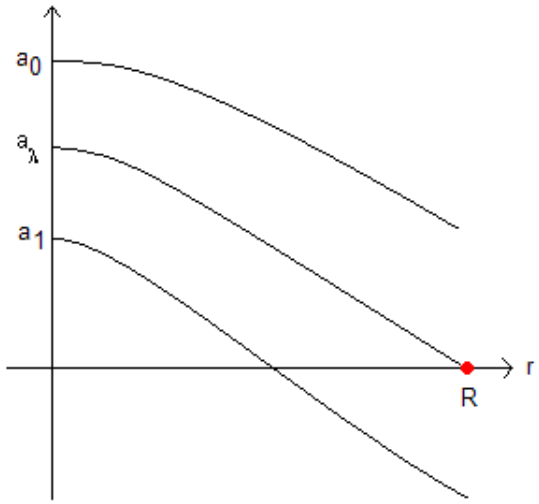

Figure 2: Graphical example of the nonlinear shooting method

4.2 The Shooting Method as a Zero Finding Problem

The iterative process outlined above is actually a root finding problem. Define $G_\lambda : \mathbb{R}^+ \to \mathbb{R}$ by $G_\lambda(a) = u_\lambda(R, a)$. $G_\lambda(a)$ takes the initial guess $a = u(0)$ and outputs the value of the corresponding solution at $r = R$, $u_\lambda(R, a)$. Our goal is to obtain a value of a, say $a = a_\lambda$, that will yield the solution that satisfies the BVP (6). In other words, we want to find a zero, a_λ, of the function G_λ.

Here is the figure of the function G_λ defined above with $\lambda = 36$ and $R = 1$ (thus the domain is the unit ball):

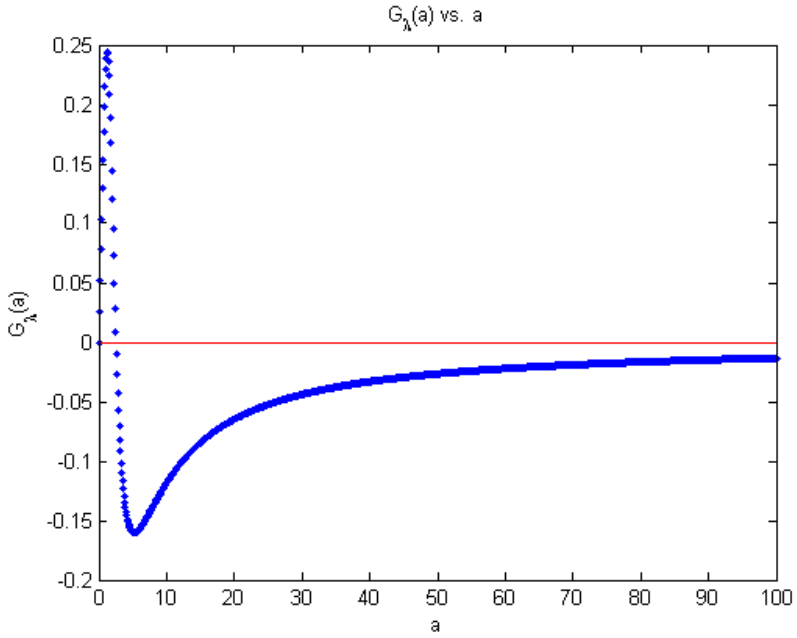

Figure 3: $G_{36}(a)$ vs. a, when $R = 1$

Note that $G_\lambda(a)$ crosses the a-axis only once over [0, 100]. This occurs at the desired value of a, say a_λ, that solves the IVP with $u(0) = a_\lambda$ and meets the boundary conditions at $r = R$, $u(R) = 0$. Also notice that, $a_\lambda = 0$ will also work. This is another zero for G_λ and when our program "shoots" a solution from this point (i.e. $u(0) = 0$), it results in the trivial solution, $u \equiv 0$. Of course, we are not interested in the trivial solution, so we always choose $a_\lambda > 0$.

We program the necessary steps of our nonlinear shooting method in **Matlab**. Matlab is a high-level language and interactive environment that enables you to perform computationally demanding tasks faster than with traditional programming languages such as C, C++, and Fortran [14].

As we said before, implementing the shooting method reduces to finding the zeros of G_λ. To do this in Matlab, we use a built-in zero finding function called **fzero**. **fzero** has two inputs: the name of the m-file where the function G_λ (see the script for G.m below) is defined and an initial guess. **fzero** first finds an interval containing the initial guess where the endpoints differ in sign. Then it searches the interval for the desired zero using a combination of the secant, bisection, and inverse quadratic interpolation methods. **fzero** returns the value of a point "near" where the function changes sign. Specifically, **fzero** returns a value a_λ for which $G_\lambda(a_\lambda) < 10^{-6}$ (close enough to zero), which is its default tolerance. If **fzero** fails to find such a point it returns "NaN".

G.m script

```
function shooting = G(a)
global lambda r0 R;
u0 = [a;-(r0/3)*(lambda*a+a^5)];
I = [r0;R];
```

```
options = odeset('RelTol',1e-6);
[r,u] = ode45('f',I,u0,options);
m = size(r,1);
shooting = u(m,1);
```

G.m returns the value of G_λ at a_λ, which is $G_\lambda(a) = u_\lambda(R, a)$, in the Matlab code. In other words, G "shoots" the solution to the IVP with initial guess $u(0) = a$. This IVP has solution $u_\lambda(\cdot, a)$. G only returns $u_\lambda(\cdot, a) atr = R$, but clearly evaluating G at a_λ requires solving an initial value problem over all of the interval [0,R], a process carried out by the instructions in lines 3 to 6 in the above script. The following sections explain in detail those instructions.

4.3 Preparing to Use ODE Solvers in Matlab

Before writing the program for the nonlinear shooting method, we have to rewrite our BVP (6) as a system containing two first order equations because Matlab can only solve first order differential equations or a system of first order differential equations. To accomplish this, we use the following change of variables:

$$\begin{aligned} u_1 = u \Rightarrow u_1' = u_2 \\ u_2 = u' \Rightarrow u_2' = u'' \end{aligned} \tag{9}$$

Now we solve for u'' in (6) and obtain

$$u_1 = u \Rightarrow u_1' = u_2 \tag{10}$$

$$u_2 = u' \Rightarrow u_2' = -\frac{2}{r}u_2 - \lambda u_1 - u_1^5. \tag{11}$$

When we set $U = [u_1; u_2]$, the ODE in our BVP (6) becomes the system of first order equations defined by

$$U' = F(r, U) = [u_2; -\frac{2}{r}u_2 - \lambda u_1 - u_1^5]. \tag{12}$$

In an m-file named **F.m**, we input the function F. Here is the content of the **F.m** file:

```
function dUdr = F(r,U)
global lambda;
dUdr = [U(2); -U(1)^5 - lambda*U(1) - (2*U(2))/r];
```

4.4 Dealing with the Singularity at $r = 0$

If asked to solve the system $U' = F(r, U)$, with $0 < r < R$, any ODE solver from Matlab will require an initial condition $U_0 = U(0) = [u_1(0); u_2(0)] = [u(0); u'(0)] = [a; 0] =$ [guess; known] and will start by evaluating F at $(r, U) = (0, U_0)$. This of course will lead to division by zero, due to the singularity present in our differential equation (now present in the second component of the vector-valued function F).

The term in the differential equation that contains the singularity, $\frac{2}{r}u'(r)$, has the indeterminant form $\frac{0}{0}$ as $r \to 0$ because of the boundary condition $u'(0) = 0$. Therefore we apply L'hôpital's to this term and get

$$\lim_{r\to 0} \frac{u'(r)}{r} = \frac{u''(0)}{1} = u''(0). \tag{13}$$

Using the result in (13), we can replace the troublesome term in ODE (6) with $u''(0)$. Solving for $u''(0)$ gives

$$u''(0) = -\frac{\lambda u(0) + u(0)^5}{3} = -\frac{\lambda a + a^5}{3}$$

where a is the initial guess for u at $r = 0$. Returning to the problem posed in vector form, we have obtained that $F(0, U_0) = [a; -(r0/3)(\lambda a + a^5)]$. For any other value of r, F continues to have the form shown in (12). Because the first step will differ from any other subsequent one as we use the ODE solvers, we decide to use **Euler's Method** to obtain the first solution point to our BVP (6), say U at some r_0 positive but small.

Euler's method is the simplest and most fundamental method for numerical integration. At any given point r in the interval, Euler's method obtains the next approximation to U, $U(r + h)$, by using a line, thus its algorithm reads: $U(r + h) = U(r) + hF(r, U(r))$. With $r = 0$ and $h = r_0$, we obtain:

$$\begin{aligned} U(r_0) &= U(0) + r_0 F(0, U(0) \\ &= U_0 + r_0 F(0, U_0) \\ &= [a; 0] + r_0[a; -\frac{r_0}{3}(\lambda a + a^5)] \\ &= [a; -\frac{r_0}{3}(\lambda a + a^5)] \end{aligned}$$

We choose the step size to be $r_0 = 10^{-10}$. Euler's method is not the most accurate. So, we use it in a single step, to pass from $r = 0$ to $r = r_0$, where the step size r_0 is chosen small enough to minimize the error introduced by the method, but positive to get away from zero.

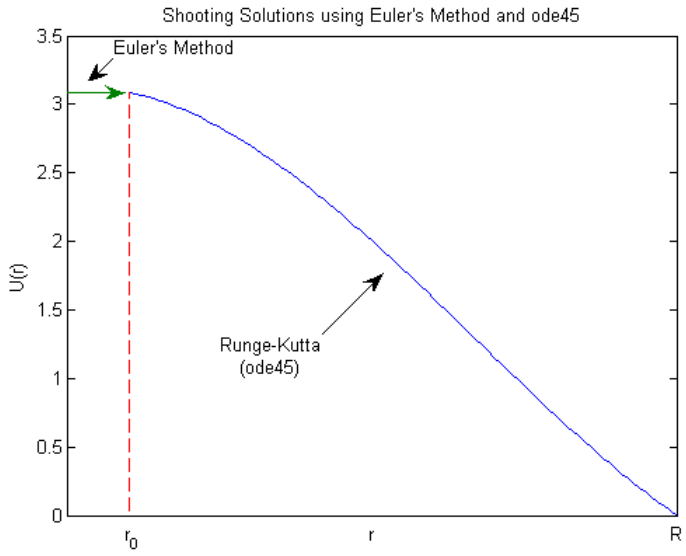

Figure 4: Note: r_0 is not drawn to scale. In reality, the difference in that first step is not noticeable by the human eye.

To solve our differential equation over the interval $[r_0, R]$ we use **ode45**. **ode45** is a standard ODE solver in Matlab. It invokes a Runge-Kutta method, which creates more efficient calculations compared to Euler's method. Runge-Kutta uses trial step-sizes at every midpoint of an interval to cancel out lower-order error terms. **ode45** then solves the IVP

$$U' = F(r, U) = [u_2, -\frac{2}{r}u_2 - \lambda u_1 - u_1^5], \quad r_0 < r < R \tag{14}$$
$$U_0 = [a; -\frac{r_0}{3}(\lambda a + a^5)].$$

This explains lines 3 thru 6 in the script file g.m presented in section 4.2.

4.5 Matlab Code Implementing the Nonlinear Shooting Method

```
global lambda r0 rf n
r0=1e-10;
rf=2; % the radius of the ball
I=[r0;rf];
L = []; A = []; m = [1]; M = [];

   % The vectors L and A will store the values of
   % lambda and a respectively. The matrix M will store
   % the corresponding soln's to the ODE, that is, M
   % will contain all the solutions obtained by this
   % program. The vector m will store the position in M
   % where one solution ends and another begins.

fprintf(1,'Enter the number of lambdas you wish to check: ')
```

```
n = input(' ');

for i = 1:n
   fprintf(1,'Enter a value for lambda: ')
   lambda = input(' ');
   fprintf(1,'Enter a guess for the value of a: ')
   guess = input(' ');
   a=fzero('sol1',guess);
   L(i) = lambda; A(i) = a;
   u0=[a;-(r0/3)*(lambda*a+a^5)];
   [r,U] = ode45('f',I,u0);
      % [r,U] is a temporary matrix to store the
      % current sol'n. Then [r,U] is concatenated
      % to the matrix M at each step. [r,U] is
      % updated with each run through the loop.
   m = [m ; m(i) + size(r,1)];
      % the ith component of the column vector
      % m stores the number of columns of the
      % vector [r,U]
   M_temp = M;
   M = [M_temp;[r,U]];
      % this code stores all the soln's to the matrix M so
      % that they can be plotted in a graph later on
end

   % this last part of the code plots the resulting graphs
clf
hold on

for j = 1:n
   plot(M(m(j):m(j+1)-1,1),M(m(j):m(j+1)-1,2))
end

display(A) % j displays all values stored in A
```

The program has a simple scheme for computing, saving, and plotting solutions to the BVP (6). It uses a *for* loop to obtain solutions to (6), given a value for λ and an initial guess a, the value of the solution at $r = 0$ ($0 \leq r \leq R$). For convenience we will refer to a as the norm of the solution, specifically the **infinity norm**. Please note that different values for λ yield distinct solutions to (6) and that various solutions have various norms (not necessarily distinct, the norm of a solution depends not only on λ but on the domain of consideration as well). Inside the loop are two predefined Matlab functions of special significance to this program: **fzero** and **ode45**. With the initial guess for the norm, the **fzero** function calls another function defined in an m-file named **sol1**. **sol1** takes the initial guess and generates the solution using **ode45**. The output of **sol1** is the value of the solution at $r = R$. **fzero** finds the particular value for the norm of the solution that will satisfy the boundary condition at R. With the correct norm, the program proceeds to store this value in a vector A. It also

stores the value of λ you entered into another vector L. So long as the program is not run again, you can make a plot comparing the values of λ and the corresponding norms of the solutions.

This program is interactive, because it asks the user for input. First, it asks for n, the number of times the program will run through the *for* loop. Inside the *for* loop, the program asks for other input from the user as well. It asks for a value for λ and an initial guess for the norm. The initial guess for the norm can be chosen arbitrarily, but from our past experience and the conjecture concerning the behavior of solutions, we choose our guesses strategically. For example, when we study solutions in the unit ball and choose different values for λ in the interval $(\frac{1}{4}\pi^2, \pi^2)$, we notice a pattern: the closer λ is to π^2, the closer the norm is to zero, and the closer λ is to $\frac{1}{4}\pi^2$, the norm increases asymptotically to infinity. When a λ is chosen that is not close to the endpoints of this interval but somewhere in between, the norm steadily increases along the interval from right to left. Similar observations about the norm of solutions for different values of λ are discovered in the balls that we study. Therefore, when we or other researchers go on to study balls of different radii, it is important to get a "feel" for how the norm of solutions to (6) behaves for different values of λ. In other words, one should test the program for a few different λ values that are reasonably close to each other. It is safe to assume that the actual values for the norm of the solution corresponding to each λ chosen are close also. Thus chose your guesses accordingly.

4.6 Error Analysis

When we study solutions to our problem in the unit ball and choose a value of λ in the interval $(\frac{1}{4}\lambda_1, \lambda_1)$ we encounter interesting results. According to the conjecture, when we approach $\lambda_1^* = \frac{1}{4}\lambda_1 \approx 2.46$ from the right, the solution u at $r = 0$ increases asymptotically to infinity. Since it is not possible to reach the critical value λ_1^* (λ can never be λ_1^*), we can get reasonably close to it with our program. The value of a solution for λ near λ_1^* is expected to be large. With an initial guess of 1,000 or 10,000, our program tells us that $a_\lambda = 15.685$. If we choose our initial guess to be large, say $a_0 = 100,000$, **fzero** returns 103,748. This suggests that the function G_λ crosses the a_λ-axis more than once. The results for $\lambda = 2.6$, 2.5 are similar. A large a_0 gives a large a_λ, but for the other initial guesses, $a_0 = 1,000$, 10,000 **fzero** returns a value very near zero. These observations are summarized in Table (1).

λ	a_0	a_λ
2.7	1,000	15.685
2.7	10,000	15.685
2.7	100,000	103,748
2.6	1,000	$6.31 \cdot 10^{-30}$
2.6	10,000	$3.16 \cdot 10^{-30}$
2.6	100,000	103,784
2.5	1,000	$1.58 \cdot 10^{-30}$
2.5	10,000	$1.62 \cdot 10^{-27}$
2.5	100,000	103,824

Table 1: Note: relative tolerance = 10^{-3}

One possible explanation for this is that the function G_λ crosses the horizontal axis more than once. In fact this may be the case when using **ode45**'s default tolerance.

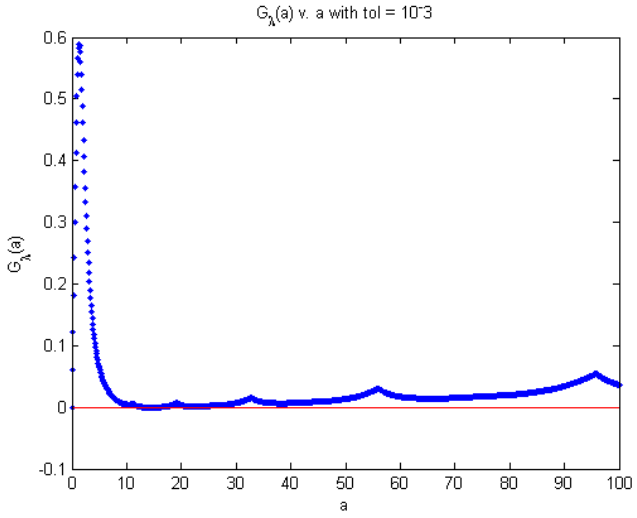

Notice that the graph of G_λ crosses or touches the horizontal axis more than once. This suggests that as we change the initial guess, **fzero** will return a root nearest the guess. Similar results are observable for the graph of G_λ when the relative tolerance of **ode45** is changed to 10^{-4} as shown in the figure below.

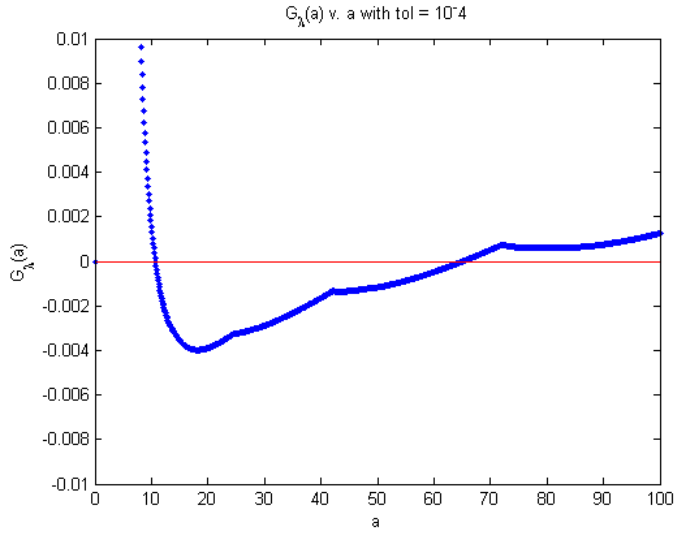

Now we want to observe the behavior of G_λ as we refine the relative tolerance of **ode45**. The next three figures show a plot G_λ where the relative tolerance is 10^{-5}, 10^{-6}, and 10^{-9}, respectively.

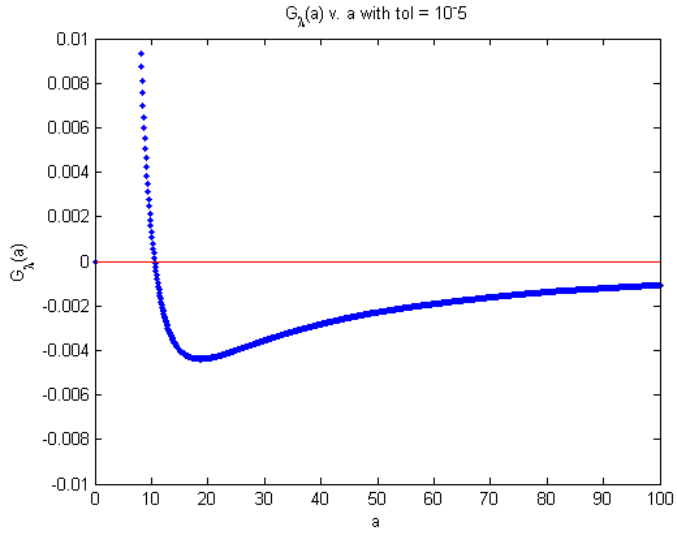

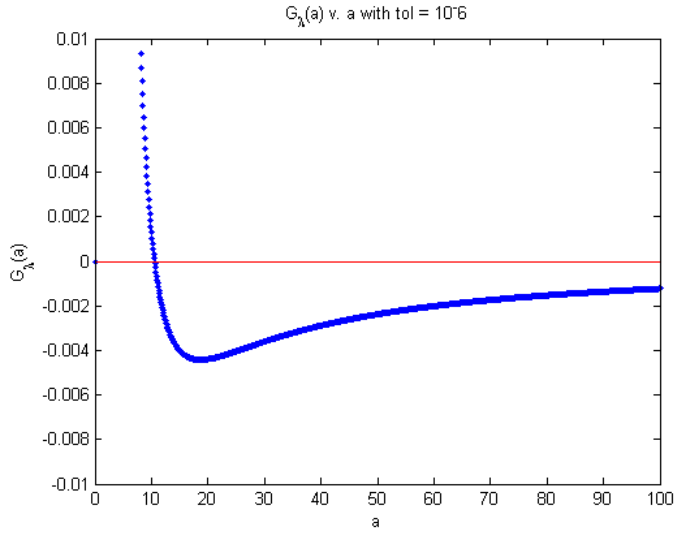

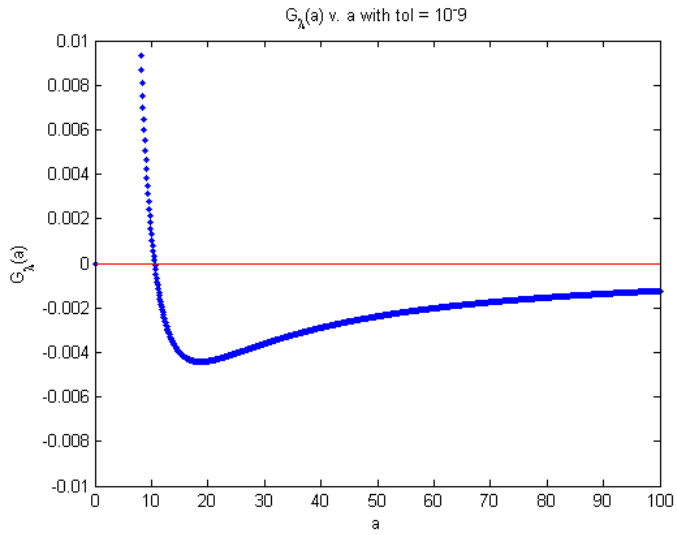

As we increase the relative tolerance for **ode45**, it becomes apparent that the function G_λ only has one zero, $a_\lambda = 15.685$, and that the function asymptotically approaches the a-axis from below. This behavior is depicted when we use relative tolerance 10^{-5}, 10^{-6}, and 10^{-9}. Based on these observations, we decided to change **ode45**'s default tolerance and work with a more trustable one, 10^{-6}.

Note: The asymptotic behavior of G_λ was observed for different values of λ within the first two λ intervals when working in the unit ball. Consistently, G_λ crosses the a-axis once, from positive to negative, and continues to approach the a-axis from below. Presumably, the a-axis is a horizontal asymptote for G_λ, in which case we would have the uniqueness of a_λ and therefore the uniqueness of our solutions. G_λ's observed qualitative behavior certainly provides evidence that solutions (or solution pairs) might be unique. This is not the focus of our work, but it is possible for future research.

5 Results

5.1 Findings and Observations

5.1.1 Eigenfunctions and Eigenvalues for a general R

Due to the problem's high nonlinearity, we follow standard procedures to linearize our PDE (5) and ODE (6). By removing the nonlinear terms, we find the eigenvalues that guide us in using our boundary value problem solver. Specifically, we know what values of λ to consider when shooting solutions with out BVP solver.

In order to find the generalized eigenfunctions and eigenvalues for any given R, we have to linearize our equations. Therefore, under symmetry assumptions:

Linearized Partial Differential Equation

$$\begin{aligned} -\Delta u &= \lambda u \text{ in } B \\ u &= 0 \quad \text{on } \partial B \end{aligned}$$

Linearized Ordinary Differential Equation

$$\begin{aligned} -u'' - \frac{2}{r}u' &= \lambda u, 0 < r < R \\ u'(0) &= 0 \\ u(R) &= 0 \end{aligned} \tag{15}$$

Based on the solution for $R = 1$, we naturally guess a similar solution that depends on R, say

$$u_j(r) = \frac{1}{r}\sin\left(\frac{j\pi r}{R}\right)$$

Next we find the first and second derivatives of the guess solution:

$$u' = \frac{1}{r}\cos\left(\frac{j\pi r}{R}\right)\left(\frac{j\pi}{R}\right) - \frac{1}{r^2}\sin\left(\frac{j\pi r}{R}\right)$$

$$u'' = -\frac{1}{r}\sin\left(\frac{j\pi r}{R}\right)\left(\frac{j\pi}{R}\right)^2 - \frac{2}{r^2}\cos\left(\frac{j\pi r}{R}\right)\left(\frac{j\pi}{R}\right) + \frac{2}{r^3}\sin\left(\frac{j\pi r}{R}\right)$$

Then we check to see if the guess solution satisfies the boundary conditions:

$$u(R) = \frac{1}{R}\sin(j\pi) = 0$$

$$u_j'(0) = \lim \frac{\left(\frac{j\pi r}{R}\right)\cos\left(\frac{j\pi r}{R}\right) - \sin\left(\frac{j\pi r}{R}\right)}{r^2} = \frac{0}{0}$$

Because we can not divide by zero, we must use L'hôpital's rule to solve for $u_j'(0)$.

$$\begin{aligned} u_j'(0) &= \frac{\left(\frac{j\pi}{R}\right)\cos\left(\frac{j\pi r}{R}\right) + r\sin\left(\frac{j\pi r}{R}\right)\left(\frac{j\pi}{R}\right)^2 - \cos\left(\frac{j\pi r}{R}\right)\left(\frac{j\pi}{R}\right)}{2R} \\ &= \frac{\frac{j\pi}{R} - 0 - \frac{j\pi}{R}}{R} \\ &= 0 \end{aligned}$$

Since our guess solution satisfies the two boundary conditions, we are certain that we have the correct eigenfunctions along with the associating eigenvalues:

Eigenfunctions:

$$u_j(x) = \frac{1}{|x|}\sin(\frac{j\pi|x|}{R}) \quad \text{or} \quad u_j(r) = \frac{1}{r}\sin(\frac{j\pi r}{R}) \tag{16}$$

Eigenvalues:

$$\lambda_j = (\frac{j\pi}{R})^2, \quad j = 1, 2, \ldots \tag{17}$$

5.1.2 Generalized Conjecture

We are initially given the list of known results (section 2.2) and the conjecture for the unit ball, Conjecture 1. Upon verifying the conjecture for higher λ_j intervals, we go on to study other sized balls besides the unit ball and discover a generalization of the conjecture that works for different sized balls. Thus, the conjecture becomes the general form

> **Generalized Conjecture**: Let $R > 0$ and $\lambda_j = (\frac{j\pi}{R})^2, j \in \mathbb{N}$, be the eigenvalues for the linearized problem associated with (6) and $\lambda_j^* = (1 - \frac{1}{2j})^2\lambda_j$. For every $\lambda \in (\lambda_j^*, \lambda_j)$, there is a solution pair $\{u_\lambda, -u_\lambda\}$. Moreover, $\|u_\lambda\|_\infty \to 0$ as $\lambda \to \lambda_j^-$ and $\|u_\lambda\|_\infty \to \infty$ as $\lambda \to (\lambda_j^*)^+$.

5.1.3 Bump in the road

As stated before, we first study a given conjecture that states that $\lambda_j^{1/2} - (\lambda_j^*)^{1/2} = \frac{\pi}{2}$ for $R = 1$. Since we know that $\lambda_j = (\frac{j\pi}{R})^2$, we can solve for $\lambda_j^* = \left(1 - \frac{1}{2j}\right)^2\lambda_j$.

Because we want to see how solutions of the ODE (6) behave in other domains besides the unit ball, we generalize our eigenfunction and eigenvalue formulas so as to depend on R. At first, we only use the generalized λ_j formula, $\lambda_j = (\frac{j\pi}{R})^2$, to plug into the λ_j^* formula. After a few simulations, we realize that we may have been using the wrong conjecture because we are not taking into consideration that the λ_j^* formula is missing an R term. So we return to the conjecture and solve for a general λ_j^* formula so that it contains an R term, $\lambda_j^* = \left(1 - \frac{R}{2j}\right)^2\lambda_j$, where $\lambda_j = \left(\frac{j\pi}{R}\right)^2$.

After running numerous simulations to test the validity of both conjectures, the λ_j^* formula for the unit ball appears to be valid even for other sized balls whereas the general formula does not appear to work. Thus, we continue to use the original λ_j^* formula and do not use the general formula.

5.1.4 In the Long Run

This section goes into a few details about what happens in the long run to λ_j, λ_j^*, and $(\lambda_j - \lambda_j^*)$.

Given $\lambda_j = (\frac{j\pi}{R})^2, j \in \mathbb{N}$, and $\lambda_j^* = (1 - \frac{1}{2j})^2\lambda_j = (1 - \frac{1}{2j})^2(\frac{j\pi}{R})^2 = (j - \frac{1}{2})^2\frac{\pi^2}{R^2}$,

1. When R is fixed,

   (a) $\lim_{j\to\infty}(\lambda_j^*) = \lim_{j\to\infty}[(j - \frac{1}{2})^2\frac{\pi^2}{R^2}] = \infty$

   (b) $\lim_{j\to\infty}(\lambda_j) = \lim_{j\to\infty}[(\frac{j\pi}{R})^2] = \infty$

   (c)

$$\begin{aligned}
\lim_{j\to\infty}(\lambda_j - \lambda_j^*) &= \lim_{j\to\infty}\left[\lambda_j - \left(1 - \frac{1}{2j}\right)^2\lambda_j\right] \\
&= \lim_{j\to\infty}\left[\left(\lambda_j \quad 1 - \left(1 - \frac{1}{2j}\right)^2\right)\right] \\
&= \lim_{j\to\infty}\left[\left(\frac{j\pi}{R}\right)^2\left(1 - \left(1 - \frac{1}{j} + \frac{1}{4j^2}\right)\right)\right]\left(\right. \\
&= \left(\frac{j\pi}{R}\right)^2\lim_{j\to\infty}\left[\left(1 - 1 + \frac{1}{j} - \frac{1}{4j^2}\right)\right]\left(\right. \\
&= \frac{\pi^2}{R^2}\lim_{j\to\infty}\left[\left(j - \frac{1}{4}\right)\right]\left(\right. \\
&= \infty
\end{aligned}$$

   Therefore, when R is fixed, λ_j^*, λ_j, and the length of the intervals $(\lambda_j - \lambda_j^*)$ increase without bound as j increases. In other words, the higher the λ_j interval, the λ_j and λ_j^* values become larger and further apart. In terms of the bifurcation diagram, the bifurcation branches become larger and more distant from each other as j increases.

2. When j is fixed,

   (a) $\lim_{R\to\infty}(\lambda_j^*) = \lim_{R\to\infty}[(j - \frac{1}{2})^2\frac{\pi^2}{R^2}] = 0$

   (b) $\lim_{R\to\infty}(\lambda_j) = \lim_{R\to\infty}[(\frac{j\pi}{R})^2] = 0$

   (c)

$$\begin{aligned}
\lim_{R\to\infty}\left(\lambda_j - \lambda_j^*\right) &= \lim_{R\to\infty}\left[\left(\frac{j\pi}{R}\right)^2 - \left(j - \frac{1}{2}\right)^2\frac{\pi^2}{R^2}\right]\left(\right. \\
&= \lim_{R\to\infty}\left[\left(\frac{\pi^2}{R^2} \quad j^2 - \left(j - \frac{1}{2}\right)^2\right)\right] \\
&= 0
\end{aligned}$$

Therefore, when j is fixed, λ_j^*, λ_j, and the lengths of the intervals $(\lambda_j - \lambda_j^*)$ decrease as R increases. That is, as the radius of the ball gets larger, the lengths of the λ_j intervals become smaller and smaller.

3. When j is fixed,

   (a) $\lim_{R\to 0}(\lambda_j^*) = \lim_{R\to 0}[(j-\frac{1}{2})^2\frac{\pi^2}{R^2}] = \infty$

   (b) $\lim_{R\to 0}(\lambda_j) = \lim_{R\to 0}[(\frac{j\pi}{R})^2] = \infty$

   (c)

$$\begin{aligned}\lim_{R\to 0}(\lambda_j - \lambda_j^*) &= \lim_{R\to 0}\left[\left(\frac{j\pi}{R}\right)^2 - \left(j-\frac{1}{2}\right)^2\frac{\pi^2}{R^2}\right]\Bigg(\\ &= \lim_{R\to 0}\left[\frac{\pi^2}{R^2}\quad j^2 - \left(j-\frac{1}{2}\right)^2\right)\Bigg]\\ &= \infty\end{aligned}$$

   Thus, when j is fixed, λ_j^*, λ_j, and the lengths of the intervals $(\lambda_j - \lambda_j^*)$ increase as R decreases. In other words, as the radius of the ball gets smaller, the lengths of the λ_j intervals become larger and larger.
   For example, the following table gives the first three lambda values for three different R values.

$R=1$	$R=1/2$	$R=2$
$\lambda_1 = \pi^2$	$\lambda_1 = 4\pi^2$	$\lambda_1 = \frac{\pi^2}{4}$
$\lambda_2 = 4\pi^2$	$\lambda_2 = 16\pi^2$	$\lambda_2 = \pi^2$
$\lambda_3 = 9\pi^2$	$\lambda_3 = 36\pi^2$	$\lambda_3 = \frac{9\pi^2}{4}$

   When $R=2$, $\lambda_1 = \frac{\pi^2}{4}$;
   when $R=1$, $\lambda_1 = \pi^2$; and
   when $R=\frac{1}{2}$, $\lambda_1 = 4\pi^2$.

   In addition, when $R=2$, the difference between λ_1 and λ_2 is $\frac{3\pi^2}{4}$;
   when $R=1$, the difference between λ_1 and λ_2 is $3\pi^2$; and
   when $R=\frac{1}{2}$,the difference between λ_1 and λ_2 is $12\pi^2$.

4. Since the length of the intervals increase as j increases, we worried that consecutive λ_j

intervals will overlap.

$$\begin{aligned}
\lim_{j\to\infty}(\lambda_j^* - \lambda_{j-1}) &= \lim_{j\to\infty}\left[\left(1-\frac{1}{2j}\right)^2\lambda_j - \lambda_{j-1}\right]\Bigg(\\
&= \lim_{j\to\infty}\left[\left(1-\frac{1}{2j}\right)^2\left(\frac{j\pi}{R}\right)^2 - \left(\frac{(j-1)\pi}{R}\right)^2\right]\Bigg(\\
&= \frac{\pi^2}{R^2}\lim_{j\to\infty}\left[\left(1-\frac{1}{j}\right)^2(j^2) - (j-1)^2\right]\Bigg(\\
&= \frac{\pi^2}{R^2}\lim_{j\to\infty}\left[\left(1-\frac{1}{j}+\frac{1}{4j^2}\right)(j^2) - (j^2-2j+1)\right]\Bigg(\Bigg(\\
&= \frac{\pi^2}{R^2}\lim_{j\to\infty}\left[j^2 - j + \frac{1}{4} - j^2 + 2j - 1\right]\Bigg(\\
&= \frac{\pi^2}{R^2}\lim_{j\to\infty}\left[j - \frac{3}{4}\right]\Bigg(\\
&= \infty
\end{aligned}$$

Since the limit of the distance between consecutive intervals increases as j increases, the consecutive intervals will never overlap each other. In addition, the distance between them strictly increases. The closest distance between the two lambda values is when $j = 2$. This finding is important because in higher dimensions, it is found that they get closer to each other.

5.2 Graphs

Using numerical analysis, different values of λ produce various solutions to our nonlinear ODE (6). The behavior of the solutions can be positive, change sign, or even have no solution.

Matlab's nonlinear shooting method allows us to find the solution curves that would reach our target $(R, 0)$. It calculates $a_\lambda = u_\lambda(0)$, our shooting point. As we select different values of λ within each interval, we get distinct solution curves shot from different a_λ values. When we study positive solutions ($\lambda \in (\lambda_1^*, \lambda_1)$), we notice that all of them were strictly decreasing. When we study solutions that change sign ($\lambda \in (\lambda_j^*, \lambda_j)$, $j = 2, 3, \ldots$) we notice that they oscillate with decreasing amplitudes. Thus, for all of our solution curves, it holds that $\max_{0\le r\le R}|u_\lambda(r)|$ occurs at $r = 0$. In other words, $a_\lambda = u(0) = \max_{0\le r\le R}|u_\lambda(r)| = \|u_\lambda\|$. This allows us to plot, for each solution curve u_λ found, the corresponding bifurcation point (λ, a_λ). The figures labeled a_λ versus λ show bifurcation branches. So, as $\lambda \to \lambda_j^*$, the solutions tend toward infinity, which provides further evidence of there being an asymptote at λ_j^*. The following figures show the results of the nonlinear shooting method for different values of λ within each interval, and their qualitative behaviors for the distinct domains. Also, we provide results for when λ is fixed and for when λ and the R values differ.

5.2.1 Solution Curves and Bifurcation Branches for $R = 1$

The graphical results show positive solutions within the interval $(\lambda_1^* = \frac{1}{4}\lambda_1, \lambda_1)$ in the unit ball. Although only a couple of solutions are provided, we notice that different λ values produce different a_λ values. As we approach the λ_j^* value, we appear to get an asymptote at the λ_j^* approximation; thus, our results support the conjecture.

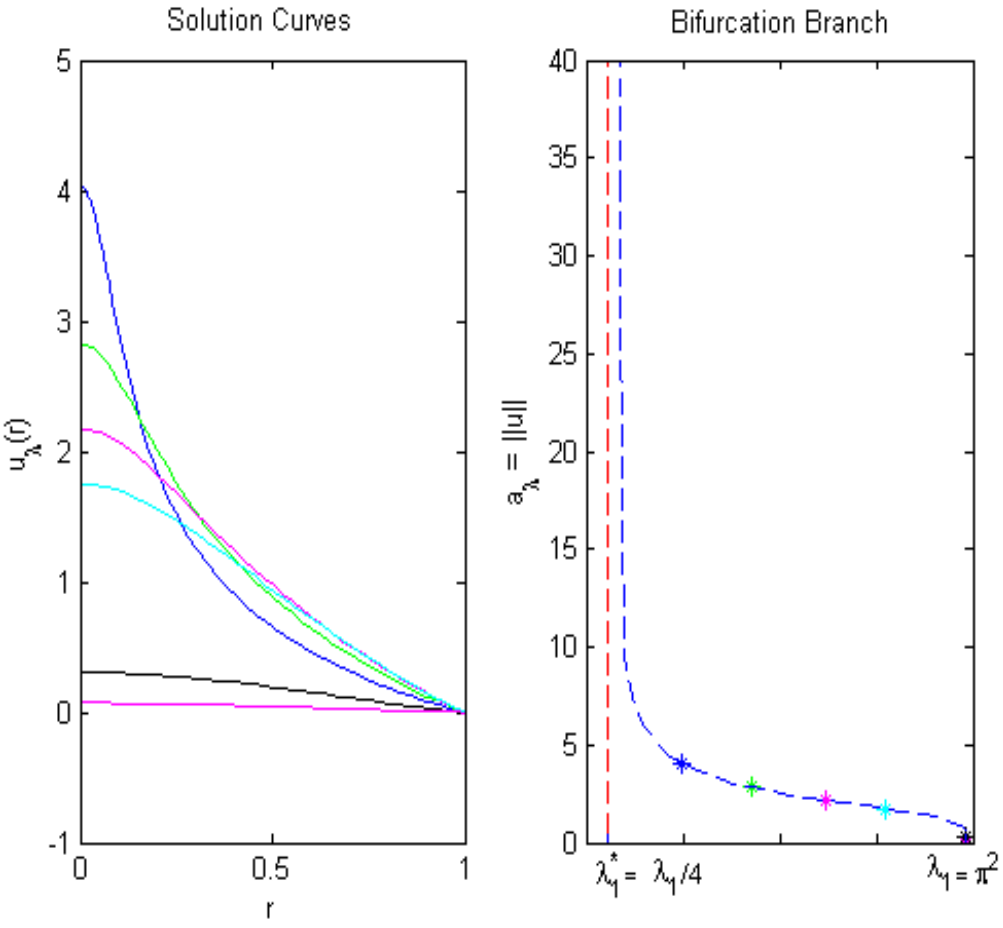

Figure 5: Solution Curves and Bifurcation Branch for $\lambda \in (\frac{1}{4}\lambda_1, \lambda_1)$ and $R = 1$

The results of this figure show an interesting outcome. Unlike the previous result with positive solutions, we now get solutions that change sign once. The qualitative behavior of the (λ_2^*, λ_2) is similar to the previous bifurcation graph which shows that as we approach λ_j^*, the bifurcation goes to infinity.

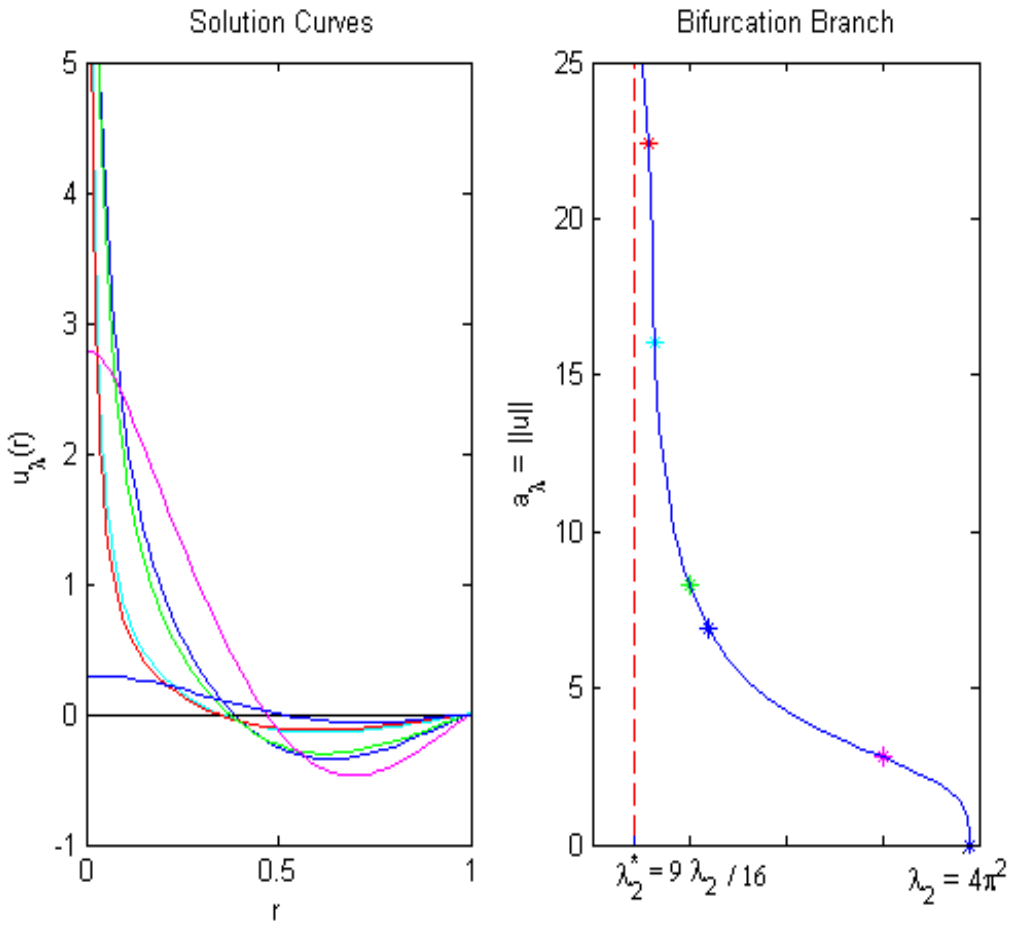

Figure 6: Solution Curves and Bifurcation Branch for $\lambda \in (\lambda_2^*, \lambda_2)$ and $R = 1$

Using the same process previously stated, we can find solutions in the interval (λ_3^*, λ_3). As we proceed with the results, pay close attention to the graph with the axes r versus u_λ because it shows that solution curves change sign twice in this case.

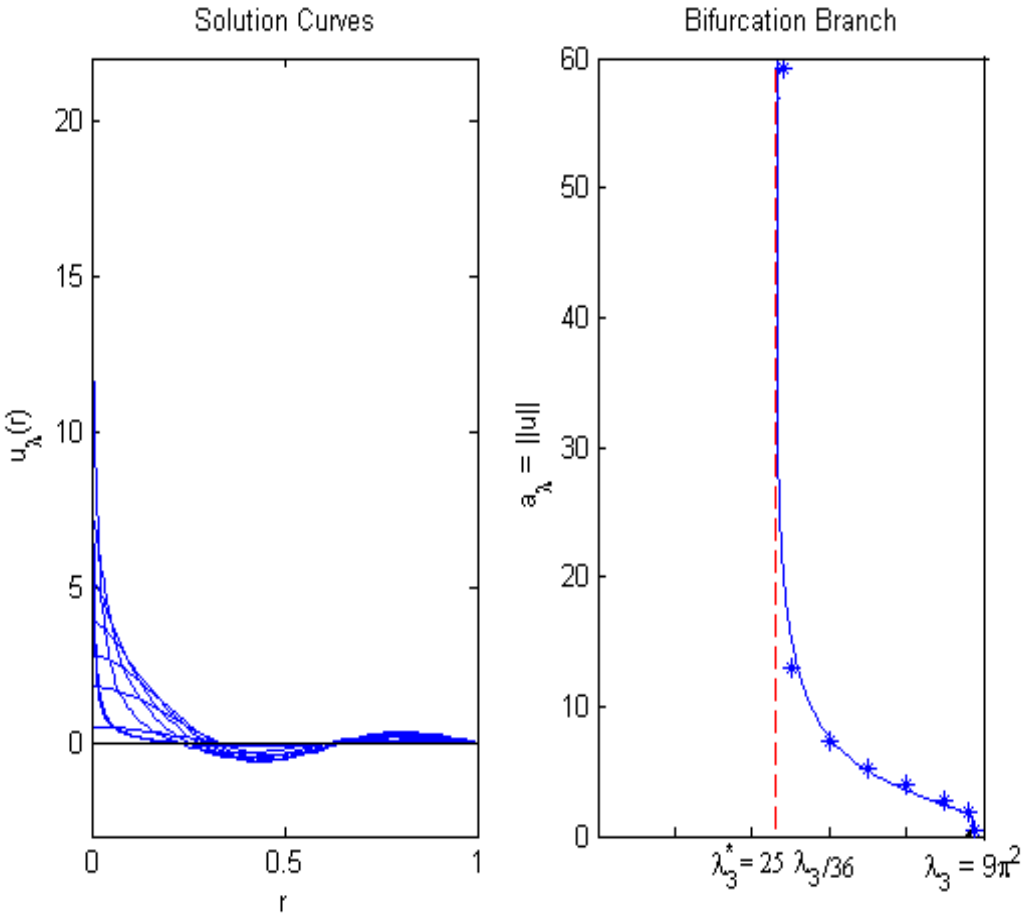

Figure 7: Solution Curves and Bifurcation Branch for $\lambda \in (\lambda_3^*, \lambda_3)$ and $R = 1$

In the interval (λ_4^*, λ_4), we have solutions that change sign three times. The bifurcation branch appears to go to infinity as λ approaches the critical value λ_4^*.

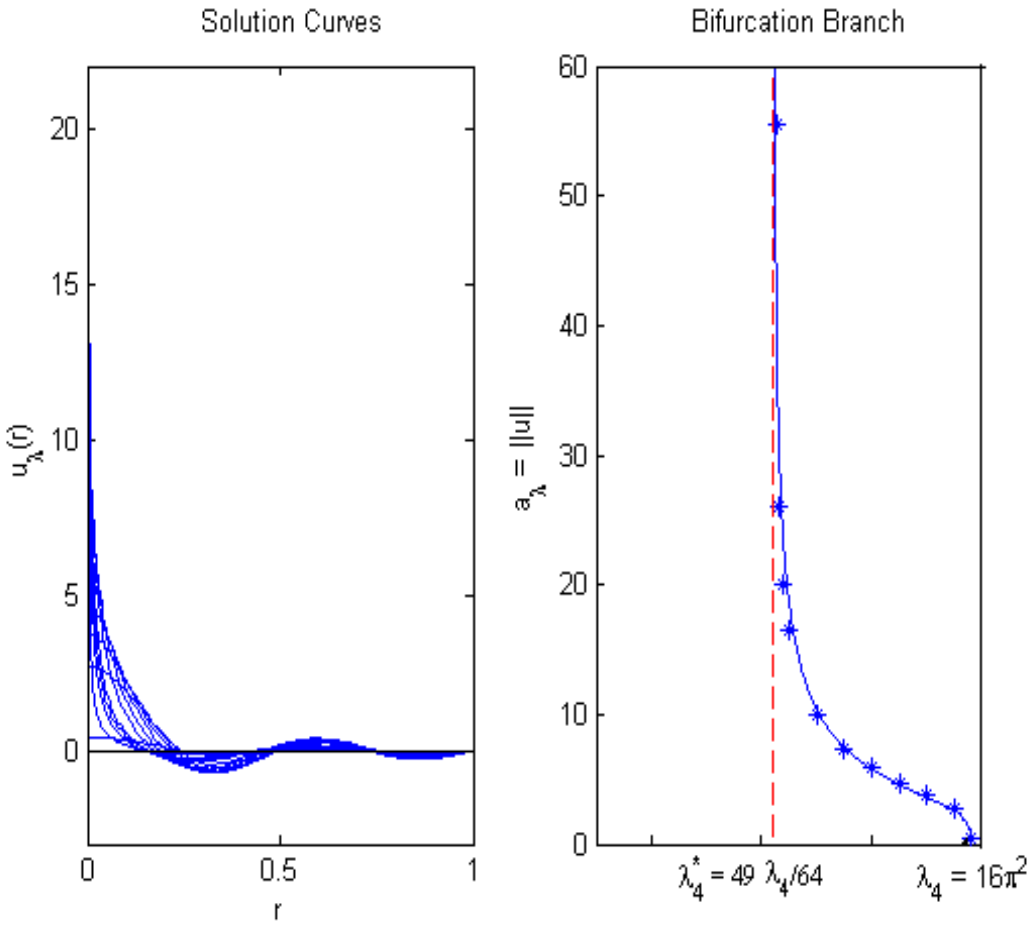

Figure 8: Solution Curves and Bifurcation Branch for $\lambda \in (\lambda_4^*, \lambda_4)$ and $R = 1$

We continue with the same process to get solutions in (λ_5^*, λ_5), except $j = 5$ in this case. We can see how the solutions change sign four times in this interval.

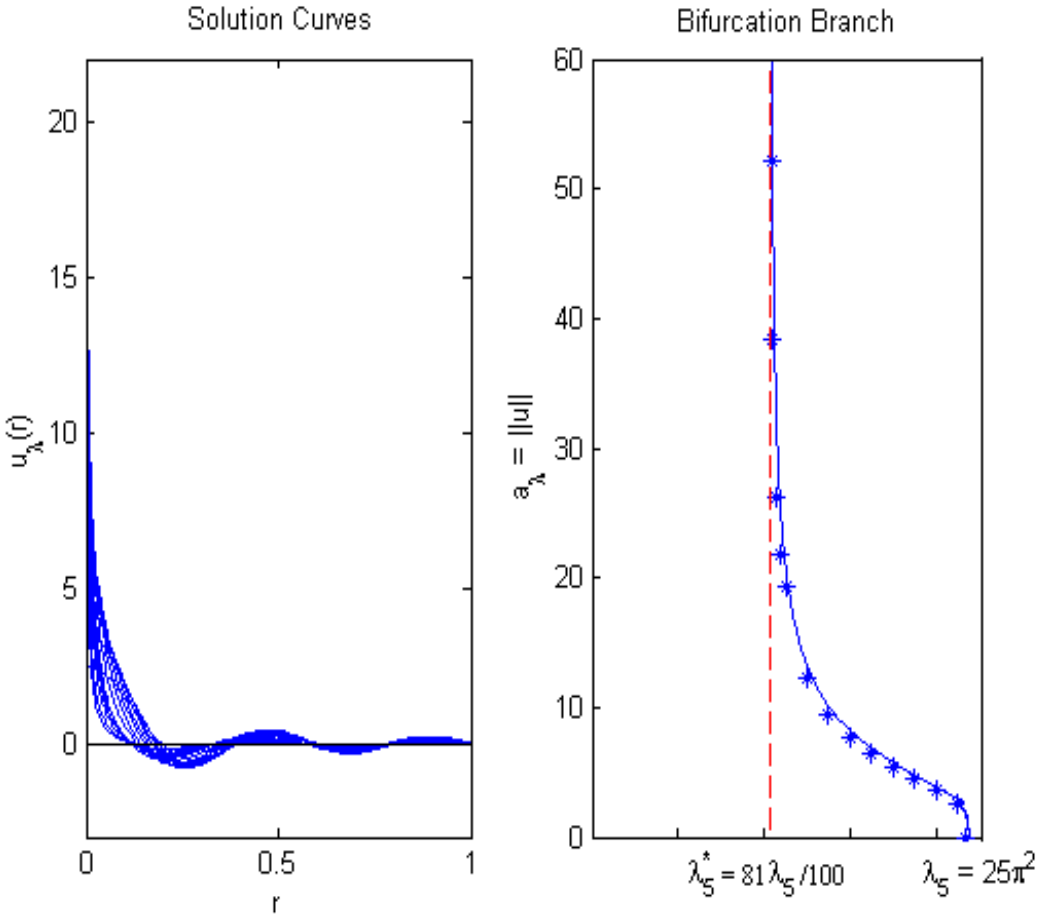

Figure 9: Solution Curves and Bifurcation Branch for $\lambda \in (\lambda_5^*, \lambda_5)$ and $R = 1$

After looking at different values of the λ_j intervals, we can conclude that the solutions change sign $j-1$ times. Based on that discovery, the solution curves change sign five times for $j=6$, which is the number of times the solution curves cross the r-axis.

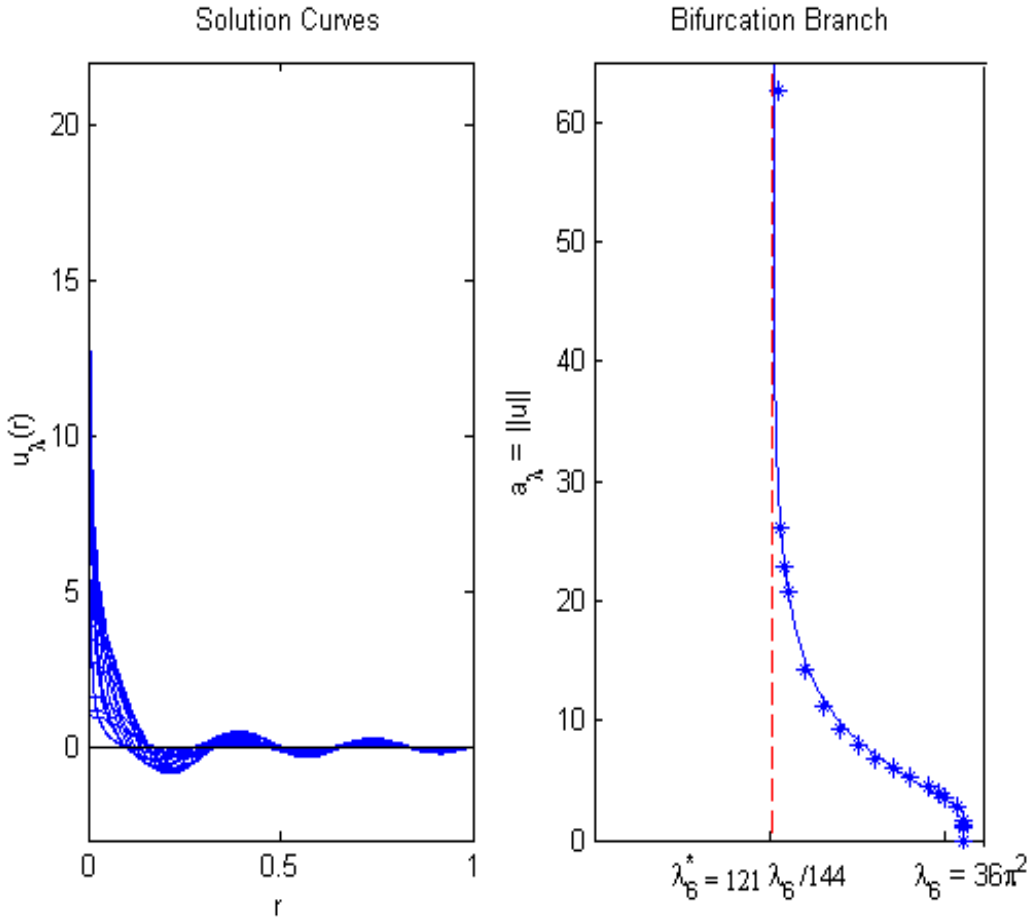

Figure 10: Solution Curves and Bifurcation Branch for $\lambda \in (\lambda_6^*, \lambda_6)$ and $R = 1$

This bifurcation diagram supports the conjecture and also shows how the different bifurcation graphs have the same qualitative behavior with an asymptote at each of their lower bounds λ_j^*.

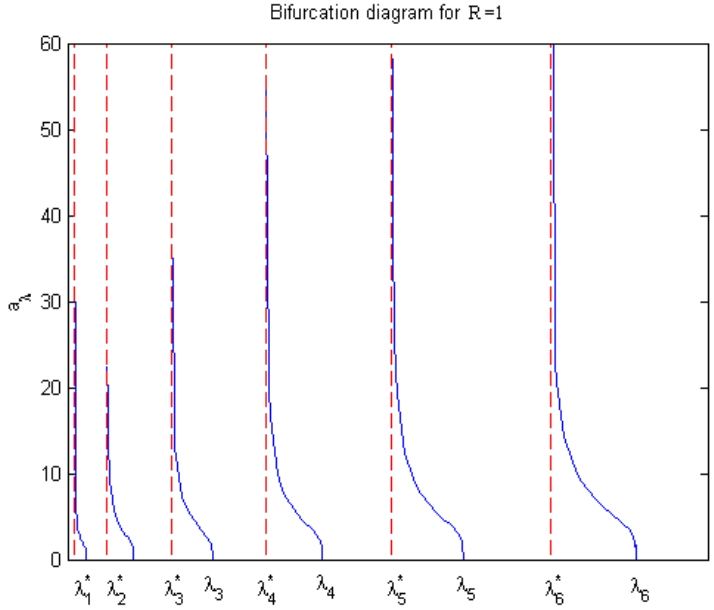

Figure 11: Bifurcation Diagram for R=1

Table for $R = 1$

Table 1 shows the values calculated for λ_j, the predicted λ_j^* and the estimated λ_j^*. The estimated λ_j^* is a close approximation to the predicted value, which helps support our conjecture but does not prove it. Furthermore, the table seems to show that there is a constant change in the length of the intervals by about 10 units as j increases.

		$R = 1$			
j	$(1-\frac{1}{2j})^2$	λ_j	Predicted λ_j^*	Estimated λ_j^*	Length of Interval
1	$\frac{1}{4}$	π^2	2.46740110027234	2.468	7.400
2	$\frac{9}{16}$	$4\pi^2$	22.20660990245106	22.300	17.270
3	$\frac{25}{36}$	$9\pi^2$	61.68502750680849	61.700	27.226
4	$\frac{49}{64}$	$16\pi^2$	120.9026539133446	121.00	37.014
5	$\frac{81}{100}$	$25\pi^2$	199.8594891220595	199.900	46.880
6	$\frac{121}{144}$	$36\pi^2$	298.5555331329531	298.600	56.800

Table 2: Note: Predicted $\lambda_j^* = (1-\frac{1}{2j})^2\lambda_j$, $\lambda_j = (j\pi)^2$, Length of Interval $= \lambda_j -$ Estimated λ_j^*

The same process to get solutions in $\lambda_1 - \lambda_6$ intervals for $R = 1$ is also used for $R = \frac{1}{4}$, $R = \frac{1}{2}$, $R = 2$, and $R = 4$. The solution curves for $R = \frac{1}{4}$, $R = \frac{1}{2}$, $R = 2$, and $R = 4$ have the same qualitative behavior as for $R = 1$: solutions change sign $j - 1$ times.

5.2.2 Bifurcation Branches and Table for $R = \frac{1}{4}$

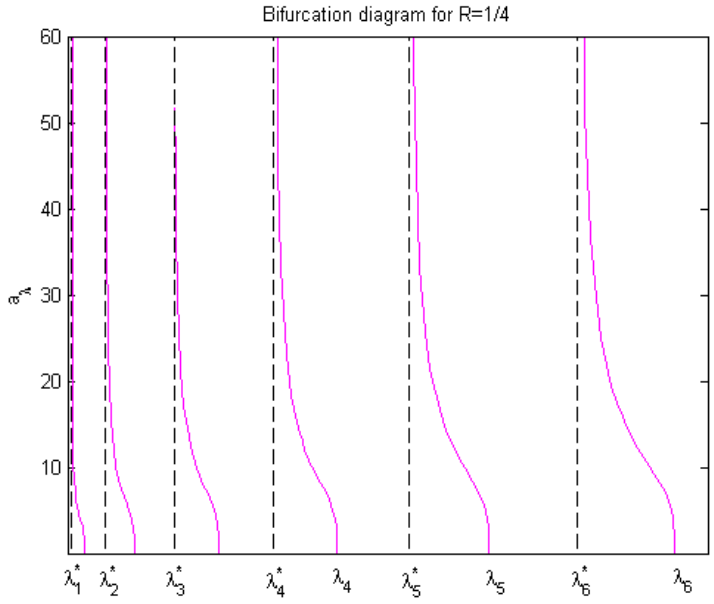

Figure 12: Bifurcation Diagram for $R = \frac{1}{4}$

Table for $R = \frac{1}{4}$

Similar to Table 1, Table 2 shows the close relationship between the predicted and estimated λ_j^* values. We see that the change in the length of the intervals increases by about 150 units as j increases.

		$R = \frac{1}{4}$			
j	$(1 - \frac{1}{2j})^2$	λ_j	Predicted λ_j^*	Estimated λ_j^*	Length of Interval
1	$\frac{1}{4}$	$16\pi^2$	39.47841760435743	43.320	114.590
2	$\frac{9}{16}$	$64\pi^2$	355.305758439217	365.800	265.760
3	$\frac{25}{36}$	$144\pi^2$	986.960440108936	1006.500	414.720
4	$\frac{49}{64}$	$256\pi^2$	1934.442462613514	1959.700	566.920
5	$\frac{81}{100}$	$400\pi^2$	3197.751825952952	3231.300	716.540
6	$\frac{121}{144}$	$576\pi^2$	4776.888530127250	4815.800	869.090

Table 3: Note: Predicted $\lambda_j^* = (1-\frac{1}{2j})^2\lambda_j$, $\lambda_j = (j\pi)^2$, Length of Interval $= \lambda_j -$ Estimated λ_j^*

5.2.3 Bifurcation Branches and Table for $R = \frac{1}{2}$

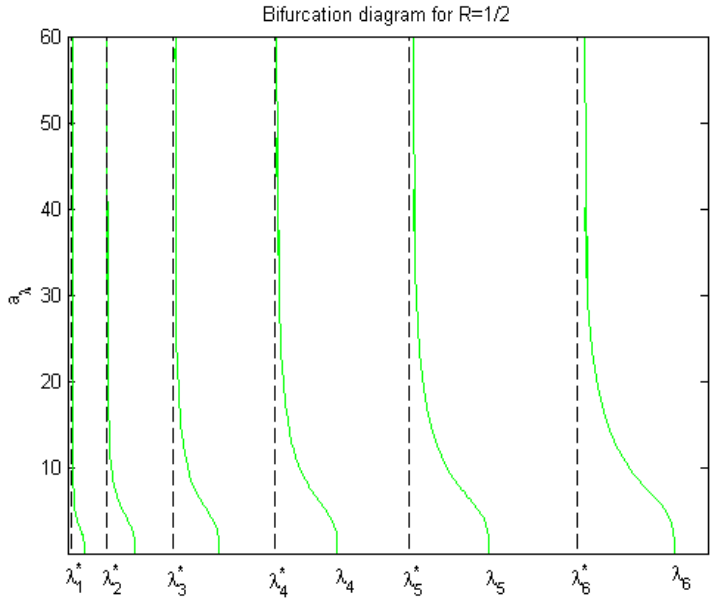

Figure 13: Bifurcation Diagram for $R = \frac{1}{2}$

Table for $R = 1/2$

The results in Table 3 continue to show the close relationship between the predicted and estimated λ_j values. The lengths of the intervals for these results show that as j increases, the change in the length of the intervals increases by about 40 units.

		$R = \frac{1}{2}$			
j	$(1 - \frac{1}{2j})^2$	λ_j	Predicted λ_j^*	Estimated λ_j^*	Length of Interval
1	$\frac{1}{4}$	$4\pi^2$	9.86960440108936	9.900	29.578
2	$\frac{9}{16}$	$16\pi^2$	88.82643960980423	89.000	68.913
3	$\frac{25}{36}$	$36\pi^2$	246.7401100272340	247.000	108.305
4	$\frac{49}{64}$	$64\pi^2$	483.6106156533786	484.000	147.654
5	$\frac{81}{100}$	$100\pi^2$	799.4379564882380	800.000	186.960
6	$\frac{121}{144}$	$144\pi^2$	1194.222132531812	1194.500	226.723

Table 4: Note: Predicted $\lambda_j^* = (1-\frac{1}{2j})^2\lambda_j$, $\lambda_j = (j\pi)^2$, Length of Interval = $\lambda_j -$Estimated λ_j^*

5.2.4 Bifurcation Branches and Table for $R = 2$

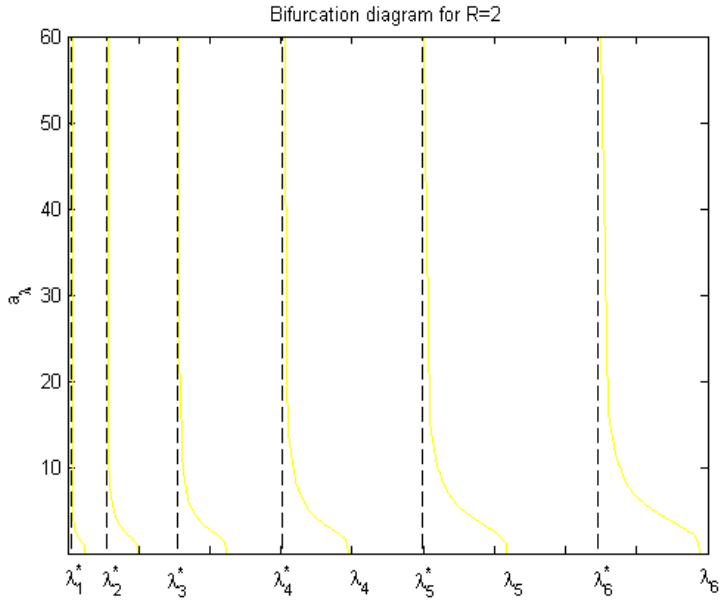

Figure 14: Bifurcation Branch for $R = 2$

Table for $R = 2$

The results for $R = 2$ again show the close relationship of the predicted and the estimated λ values. As j increases, we see that the change in the length of the intervals increases by about 2.5 units.

		$R = 2$			
j	$(1 - \frac{1}{2j})^2$	λ_j	Theoretical λ_j^*	Estimated λ_j^*	Length of Interval
1	$\frac{1}{4}$	$\frac{\pi^2}{4}$	0.61685027506	0.6765	1.7909
2	$\frac{9}{16}$	π^2	5.55165247561	5.5560	4.3136
3	$\frac{25}{36}$	$\frac{9\pi^2}{4}$	15.42125687670	15.6000	6.6066
4	$\frac{49}{64}$	$4\pi^2$	30.22566347833	30.7700	8.7080
5	$\frac{81}{100}$	$\frac{25\pi^2}{4}$	49.96487228051	49.9759	11.7091
6	$\frac{121}{144}$	$9\pi^2$	74.63888328323	74.7000	14.1264

Table 5: Note: Predicted $\lambda_j^* = (1-\frac{1}{2j})^2\lambda_j$, $\lambda_j = (j\pi)^2$, Length of Interval $= \lambda_j -$Estimated λ_j^*

5.2.5 Bifurcation Branches and Table for $R = 4$

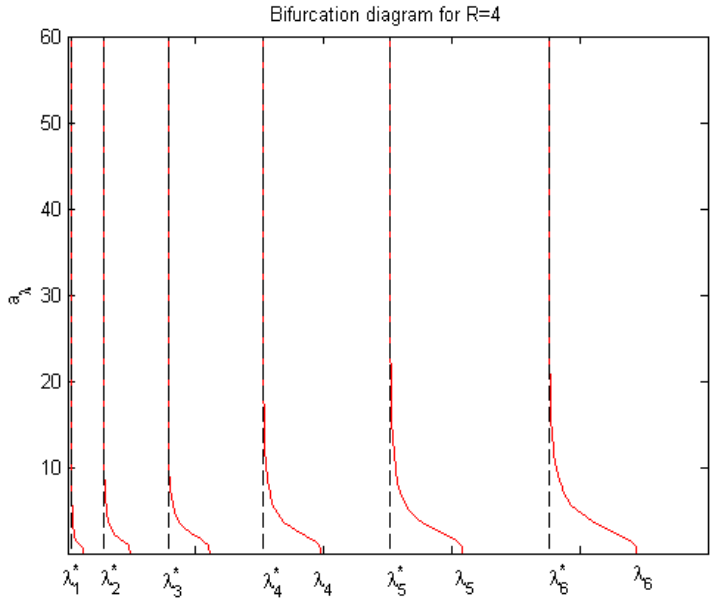

Figure 15: Bifurcation Diagram for $R = 4$

Table for $R = 4$

Once again the close relation between the predicted and estimated λ_j values is visible. For these results, the change in the length of the intervals is about 0.5 unit as j increases.

		$R = 4$			
j	$(1-\frac{1}{2j})^2$	λ_j	Predicted λ_j^*	Estimated λ_j^*	Length of Interval
1	$\frac{1}{4}$	$\frac{\pi^2}{16}$	0.15421256876702	0.168	0.449
2	$\frac{9}{16}$	$\frac{\pi^2}{4}$	1.38791311890319	1.429	1.039
3	$\frac{25}{36}$	$\frac{9\pi^2}{16}$	3.85531421917553	3.928	1.624
4	$\frac{49}{64}$	π^2	7.55641586958404	7.654	2.216
5	$\frac{81}{100}$	$\frac{25\pi^2}{16}$	12.49121807012872	12.612	2.809
6	$\frac{121}{144}$	$\frac{9\pi^2}{4}$	18.65972082080957	18.809	3.398

Table 6: Note: $\lambda_j^* = (1-\frac{1}{2j})^2\lambda_j$, $\lambda_j = (j\pi)^2$, Length of Interval = λ_j – Estimated λ_j^*

5.2.6 Additional Findings on the Tables

We first observe the changes in the lengths of the different λ_j intervals based on the last column of the tables in sections 5.2.1, 5.2.2, 5.2.3, 5.2.4, and 5.2.5 and we notice that there is a pattern in the changes in the interval lengths for each value of R that we study. For example, for $R = 1$, we notice that the change in the lengths of the intervals increases by about ten units. We go further and actually calculate the change in the length of the intervals for the different R values by using the formulas for λ_j and λ_j^*. Instead of subtracting the estimated values for λ_j^* from λ_j, we subtracted the predicted values for λ_j^* from λ_j as seen in the last columns of Tables 2, 3, 4, 5 and 6 in sections 5.2.1, 5.2.2, 5.2.3, 5.2.4, and 5.2.5.

$$
\begin{aligned}
\text{Predicted length: } \lambda_j - \lambda_j^* & \\
&= \lambda_j - \left(1 - \frac{1}{2j}\right)^2 \lambda_j \\
&= \lambda_j \quad 1 - \left(1 - \frac{1}{2j}\right)^2 \Bigg) \\
&= \left(\frac{j\pi}{R}\right)^2 \left(1 - \left(1\left(-\frac{1}{j} + \frac{1}{4j^2}\right)\right)\right(\\
&= \left(\frac{j^2\pi^2}{R^2}\right) \left(1\left(-1 + \frac{1}{j} - \frac{1}{4j^2}\right)\right(\\
&= \left(\frac{\pi^2}{R^2}\right) \left(j\left(-\frac{1}{4}\right)\right(
\end{aligned}
$$

For $R = 1$:

$$
\begin{aligned}
j^{th} \text{ interval's length:} \quad & \pi^2 \left(j - \tfrac{1}{4}\right)\Bigg(\\
(j+1)^{th} \text{ interval's length:} \quad & \pi^2 \left(j + 1 - \tfrac{1}{4}\right)\Bigg(\\
& = \pi^2 \left(j - \tfrac{1}{4}\right) + \Bigg(\pi^2 \\
& = \pi^2 \left(j - \tfrac{1}{4}\right) + 9.8696
\end{aligned}
$$

The predicted change in the length of the intervals ($\pi^2 \approx 9.8696$ units) is quite close to our approximated value of 10 units.

For any R:

$$
\begin{aligned}
j^{th} \text{ interval's length:} \quad & \tfrac{\pi^2}{R^2} \left(j - \tfrac{1}{4}\right)\Bigg(\\
(j+1)^{th} \text{ interval's length:} \quad & \tfrac{\pi^2}{R^2} \left(j + 1 - \tfrac{1}{4}\right)\Bigg(\\
& = \tfrac{\pi^2}{R^2} \left(j - \tfrac{1}{4}\right) + \Bigg(\tfrac{\pi^2}{R^2}
\end{aligned}
$$

In general, the predicted change in the length of the intervals seems to increase by increments of $\frac{\pi^2}{R^2}$, which are very close to our approximated values.

5.2.7 Bifurcation Diagrams

To better analyze the results, we provide graphs with a fixed λ value but different bifurcation branches $R = 1/4, 1/2, 1, 2$, and 4. The following graph shows the fixed λ value to be λ_1 with different R values.

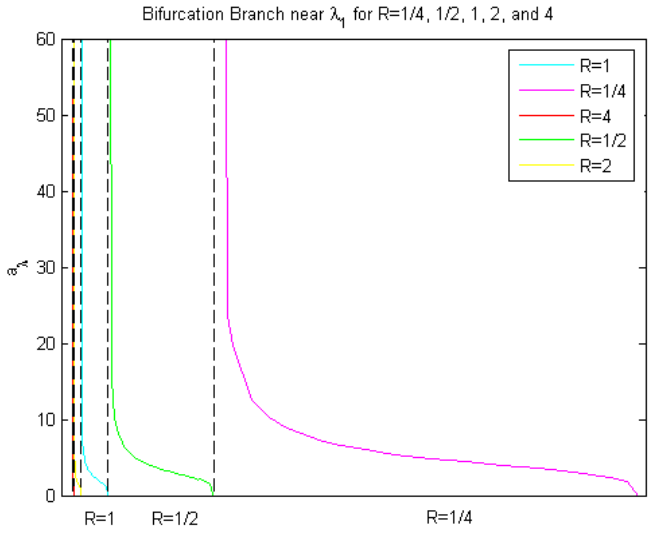

Figure 16: Bifurcation Branch for λ_1

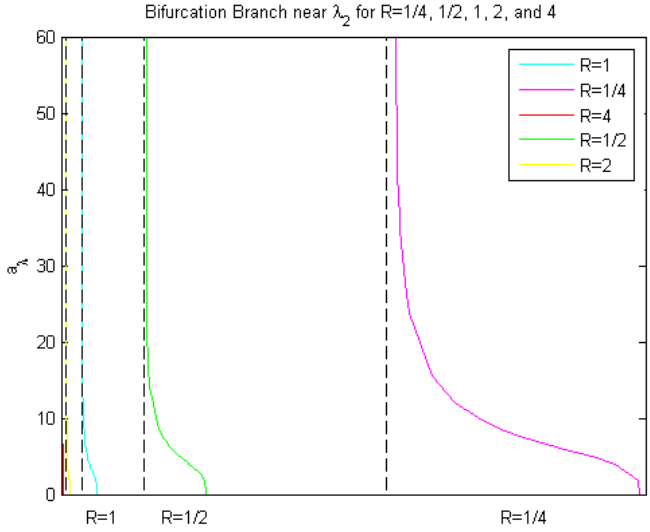

Figure 17: Bifurcation Branch for λ_2

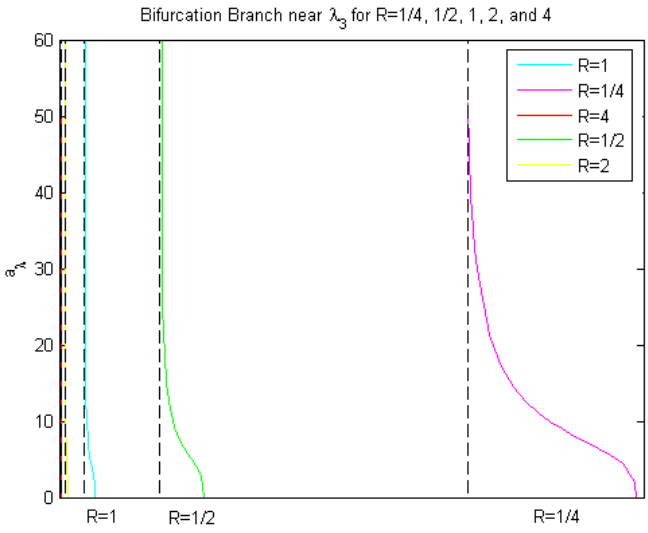

Figure 18: Bifurcation Branch for λ_3

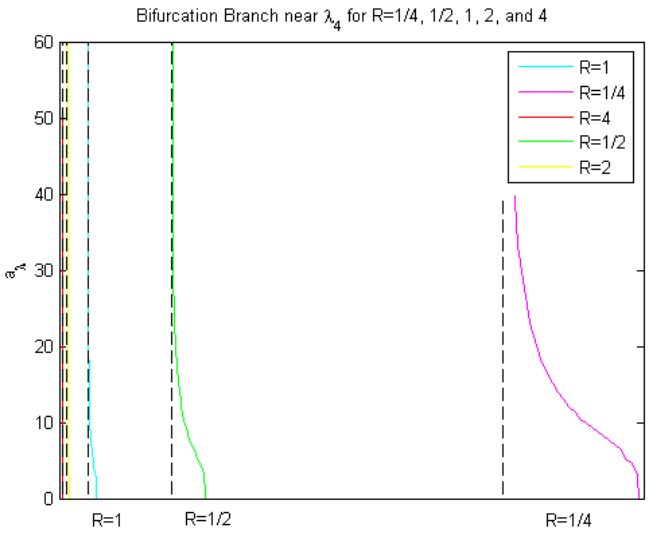

Figure 19: Bifurcation Branch for λ_4

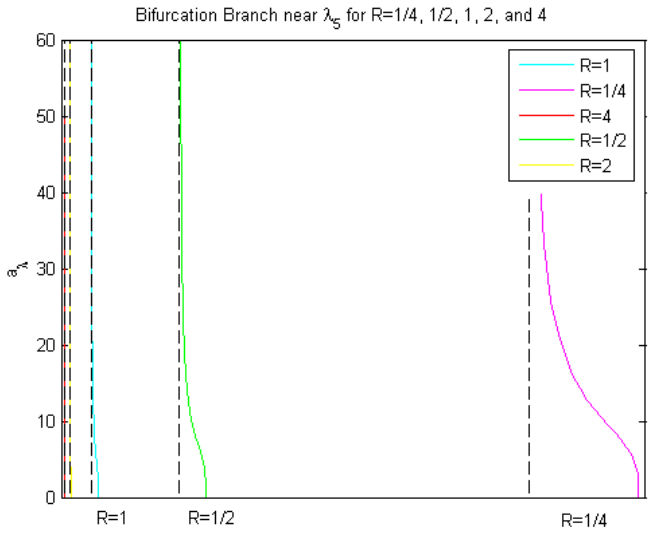

Figure 20: Bifurcation Branch for λ_5

However, the graph below shows λ_6 for all the R values. By comparing the previous bifurcation branch graphs, we notice how the length of the intervals vary.

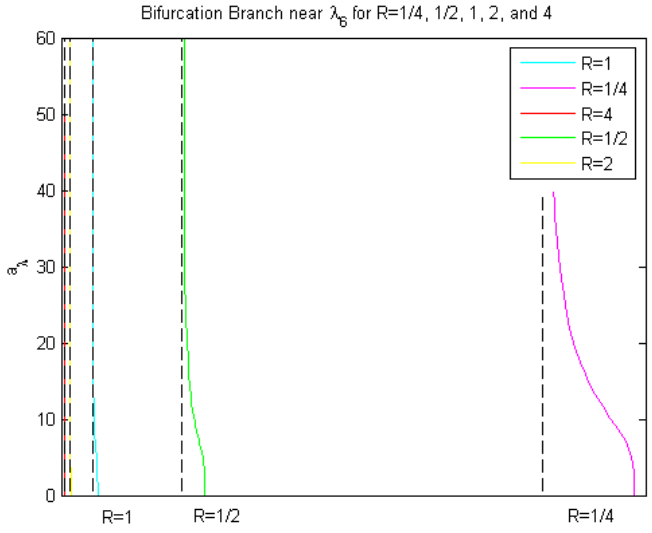

Figure 21: Bifurcation Branch for λ_6

Furthermore, we provide the different R values and the different λ_j values in the following diagrams to show the relationship between the R values and the λ_j intervals. It is difficult to see what is happening in the left side of the diagram, so we rearrange the axis to have a better look at the results.

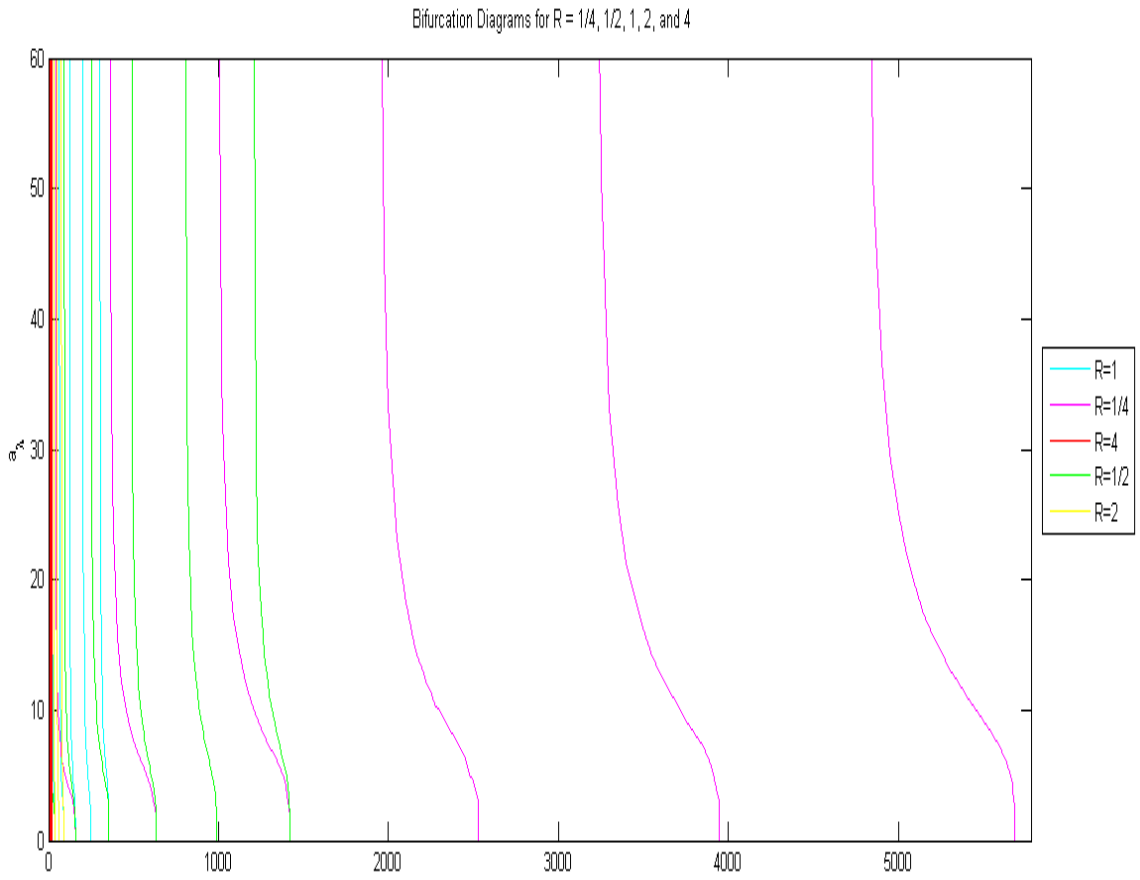

Figure 22: Bifurcation Diagram for $R = 1/4, 1/2, 1, 2, 4$

As we move our focus to the left of the diagram, we can see how some of the solution branches overlap. Also, similarities are seen between the trivial solutions or λ_j values for different R values and λ_j intervals. These solutions originate from the same point but then diverge onto separate paths.

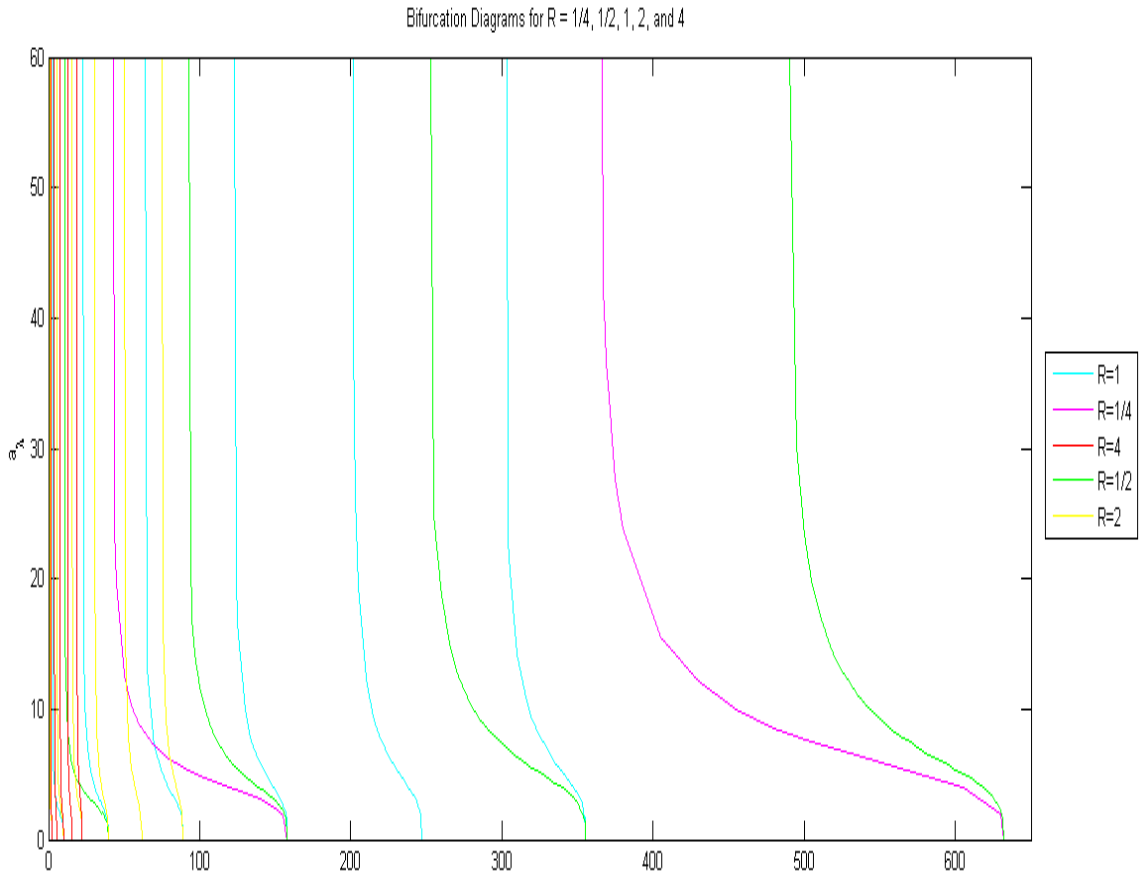

Figure 23: Bifurcation Diagram for $R = 1/4, 1/2, 1, 2, 4$

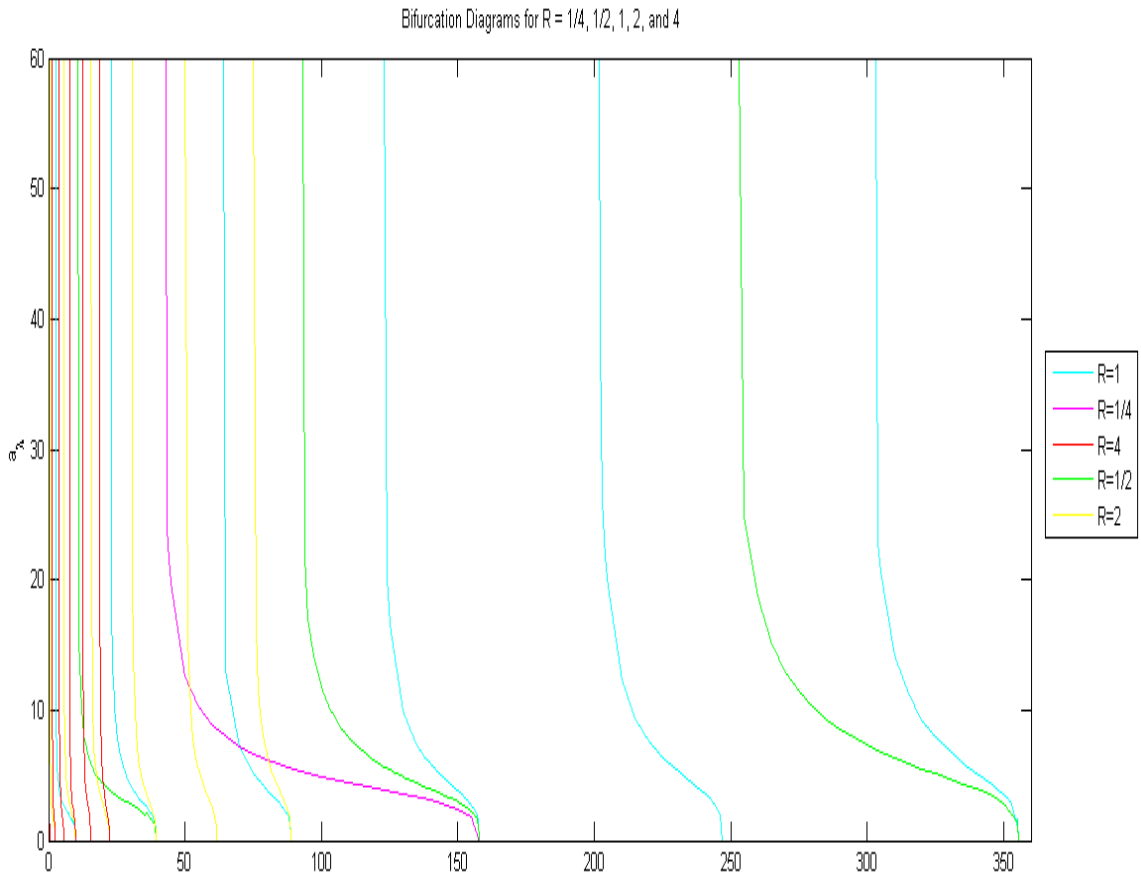

Figure 24: Bifurcation Diagram for $R = 1/4, 1/2, 1, 2, 4$

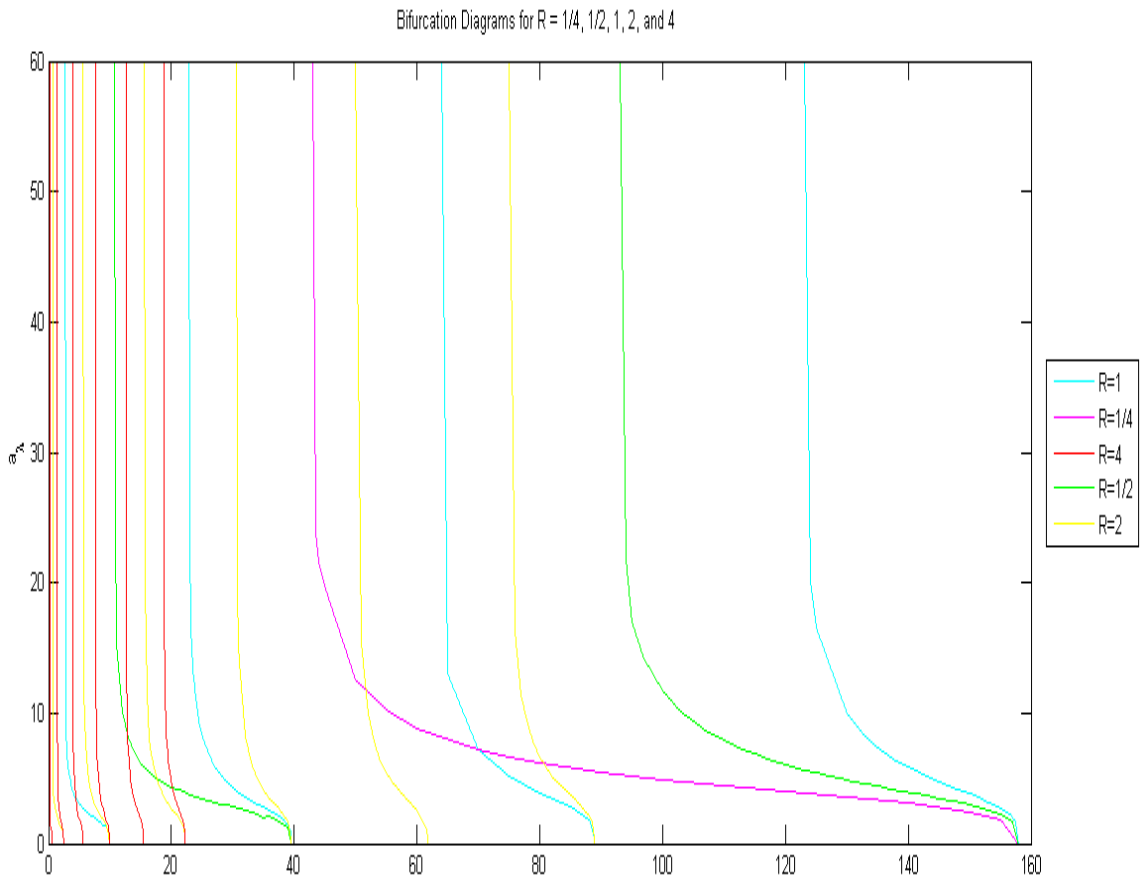

Figure 25: Bifurcation Diagram for $R = 1/4, 1/2, 1, 2, 4$

In Figure 25, the λ value at $(16\pi^2, 0) \approx (157.9, 0)$ serves as an eigenvalue for three R values. Thus, three different bifurcation branches emerge from the same λ. In this case, since $\lambda = 16\pi^2$:

$$\begin{aligned}
\text{For } R = 1, \quad \lambda_4 &= (4\pi)^2 = 16\pi^2 \\
\text{For } R = \frac{1}{2}, \quad \lambda_2 &= \left(\frac{2\pi}{\frac{1}{2}}\right)^2 = 16\pi^2 \\
\text{For } R = \frac{1}{4}, \quad \lambda_1 &= \left(\frac{\pi}{\frac{1}{4}}\right)^2 = 16\pi^2
\end{aligned}$$

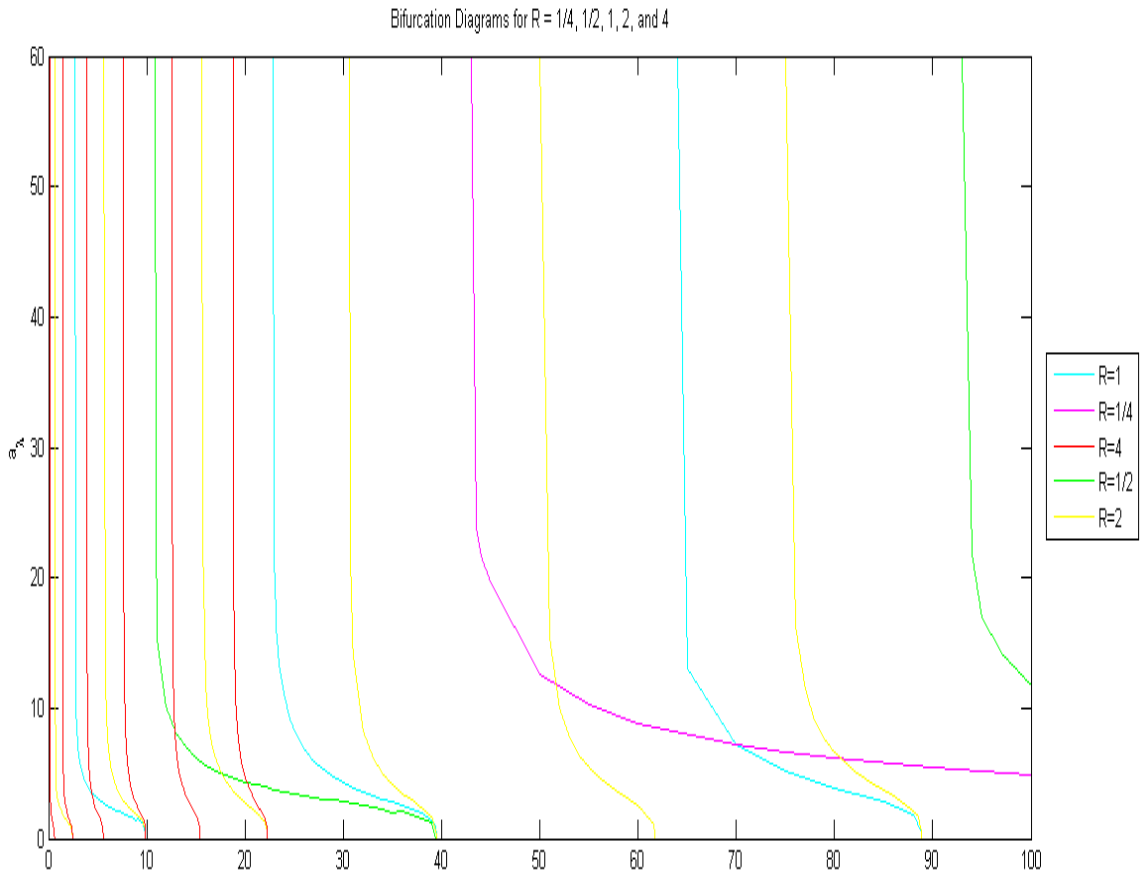

Figure 26: Bifurcation Diagram for $R = 1/4, 1/2, 1, 2, 4$

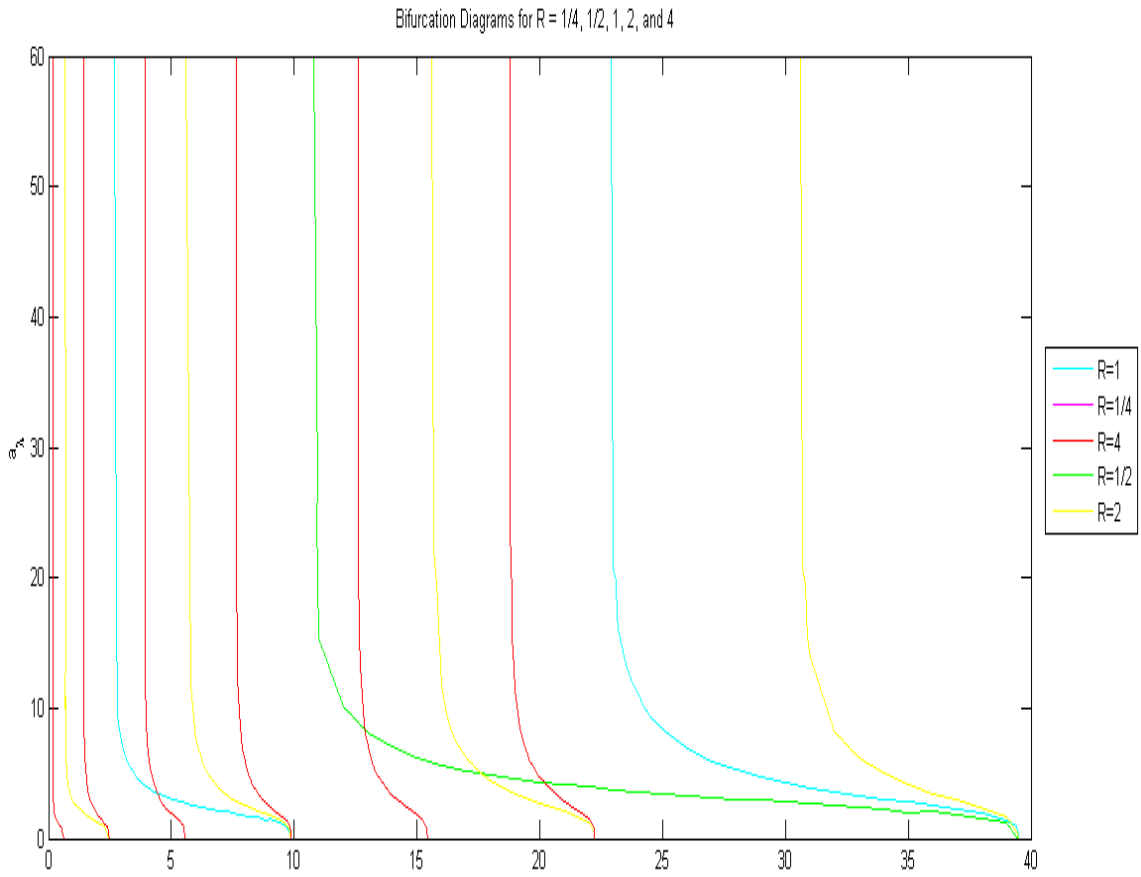

Figure 27: Bifurcation Diagram for $R = 1/4, 1/2, 1, 2, 4$

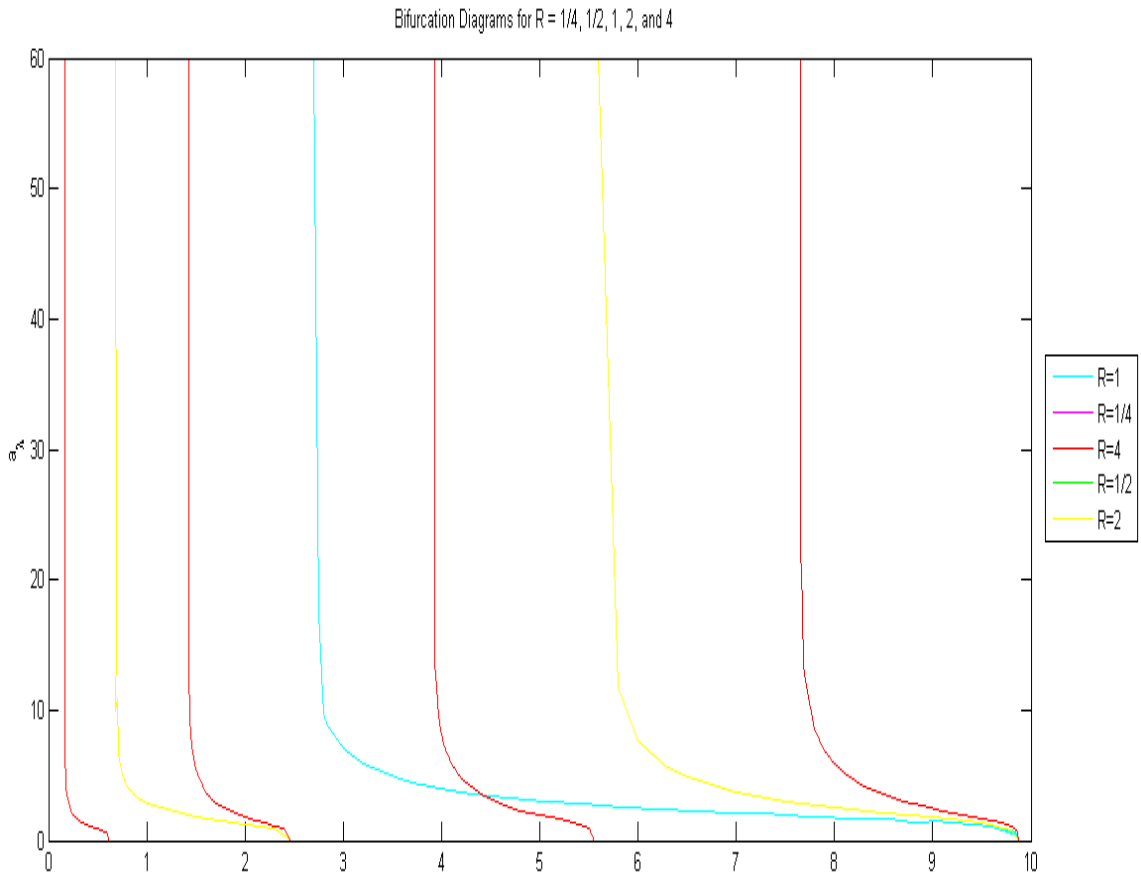

Figure 28: Bifurcation Diagram for $R = 1/4, 1/2, 1, 2, 4$

6 Conclusion

Based on our research, we discovered that the conjecture can be generalized and used for different sized balls. There appears to be an asymptote at the left bound λ_j^* of the interval (λ_j^*, λ_j) based on our numerical analysis. Also, the bifurcation branches reveal a similar qualitative behavior for different sized balls, and the solution curves indicate that the solutions change sign $j-1$ times, depending on which λ_j interval they are in. We are able to calculate what the solutions and the bifurcation branches look like in the long run and in extremely large or extremely small sized balls.

We would like to mention that the observed solution curves u_λ behave *like* the eigenfunctions $(u_j(r) = \frac{1}{r}\sin(\frac{j\pi r}{R}))$ for values of λ near λ_j. As λ approaches λ_j^*, the shape of solution curves *degenerate* and appear to approach an L-form: the value of the solution at $r = 0$ tends to ∞; the solution drops dramatically and crosses the r-axis at a value r that tends to 0; and the amplitude of the oscillations $(j-1)$ over the interval $(0, R)$ tend to 0.

As it was pointed out in the beginning of our study, the exponent $p = \frac{n+2}{n-2}$ brings forth many interesting phenomena involving the existence and nonexistence of solutions [6] to

$$-\Delta u = |u|^{p-1}u + \lambda u \text{ in } \quad , \quad u \not\equiv 0 \text{ in } \quad , \quad u = 0 \text{ on } \partial \quad .$$

The difficulty of this problem in dimension $n = 3$ has led researchers to study our problem in higher dimensions. Throughout the duration of our research, we found a paper that presented a sixteen-lemma-computer-assisted proof to prove that in dimension $n = 4$, the second bifurcation branch does not intersect the preceding eigenvalue [11]. With our conjecture, we can be certain that *none* of the bifurcation branches emanating from the bifurcation points $(\lambda_j, 0)$, $j \in \mathbb{N}$, will intersect the preceding eigenvalue. Another paper found solves our problem for some exponent slightly greater than five (i.e. $p + \epsilon$) [13] and again it confirms that our problem in its original form is harder.

7 Future Research

1. Try to use a comparison theorem [18] to trap solutions of (6) in a closed region. This could guarantee the existence of solutions as well as lower and upper bounds for the solutions. A first attempt is to compare our differential equation with

   - Lane-Emden
   $$u'' + \frac{2}{r}u' + u^5 = 0$$
   - Bessel
   $$u'' + \frac{1}{r}u' + (1 - \frac{\nu^2}{r^2})u = 0$$
   - Mathieu
   $$u'' + (\lambda - 2qcos(2r))u = 0$$

2. Prove our conjecture that

$$\begin{aligned} -\Delta u = u^5 + \lambda u \text{ in } B \\ u \not\equiv 0 \text{ in } B \\ u = 0 \text{ on } \partial B, \end{aligned}$$

where $B(0,R) \subset \mathbb{R}^3$, $R > 0$, has pairs of radially symmetric solutions, $\{u_\lambda, -u_\lambda\}$, $\forall\ \lambda \in (\lambda_j^*, \lambda_j)$, with $\lambda_j^* = (1 - \frac{1}{2j})^2 \lambda_j$, and $\lambda_j = (\frac{j\pi}{R})^2$. Moreover, solutions change sign $j-1$ times over the interval $(0,R)$. From the point of view of bifurcations, $\|u_\lambda\| \to 0$ as $\lambda \to \lambda_j$ and $\|u_\lambda\| \to \infty$ as $\lambda \to \lambda_j^*$.

- Are these solution pairs unique?

3. Study the partial differential equation instead of the ordinary differential equation.

- Are all solutions in the ball radially symmetric?

4. Find solutions of

$$\begin{aligned} -\Delta u = |u|^{p-1}u + \lambda u \text{ in} \\ u \not\equiv 0 \text{ in} \\ u = 0 \text{ on } \partial \end{aligned}$$

when is a domain other than the ball in $\mathbb{R}^n$.

- For instance, star-shaped domains other than the ball.

5. Can we extend our approach to other dimensions?

A Appendix

In this section we collected varied information that is connected, directly or indirectly, to our problem of study.

A.1 Bifurcation

It represents the sudden appearance of a qualitatively different solution for a nonlinear system as some parameter is varied.

A.2 Calculus of Variations

A branch of mathematics that generalizes finite-dimensional calculus to minimizing functions of functions, or functionals, in an infinite-dimensional case. Setting the first variation of a functional $\Phi[u] = \int\left(f(u, u', x)\, dx$ equal to zero, $\delta\Phi = 0$, results in the so-called Euler-Lagrange equation(s)$\right($which has the form

$$\frac{\partial f}{\partial u} - \frac{d}{dx}\frac{\partial f}{\partial u} = 0.$$

For example, the PDE

$$-\Delta u = |u|^{p-1}u + f(x, u)\text{in}$$

is the Euler-Lagrange equation for the functional

$$\Phi(u) = \frac{1}{2}\int\left(|\nabla u|^2 - \frac{1}{p+1}\int |u|^{p+1} - \int\left(F(x, u),\right.\right.$$

where $F(x, u) = \int_0^u\left(f(x, t)dt.\right.$ Thus, the solutions u of the PDE are minimizers for the functional Φ.

A.3 Elliptic Di erential Equation

If $D[u] = \Sigma_{i,j}a_{ij}(x)u_{x_ix_j} + \Sigma_k b_k(x)u_{x_k} + cu$, then D is called elliptic if and only if for every x, all the eigenvalues of the matrix $(a_{ij})_{ij}$ are positive and the matrix is symmetric. For example, if $D = \Delta$ in 3-D, then $b_k = 0$, $a_{ij} = 0$ if $i \neq j$, and $a_{ii} = 1$. Thus, the above matrix becomes a diagonal matrix with all the diagonal entries equal to 1.

A.4 General Theory of Relativity

Albert Einstein's general theory of relativity substitutes the idea of gravity with that of the geometry of space. This theory proposes that matter tells space-time how to curve, and curved space tells matter how to move. The mathematics behind this theory comes from Einstein's field equations, which are ten coupled hyperbolic-elliptic nonlinear partial differential equations. Theoretically, these equations can be used to describe all possible space-time scenarios. For a mathematician though, the difficulty lies in the equations being nonlinear and coupled. So, researchers are always led to restrict their calculations to simpler, and more manageable systems.

Einstein discovered that in Riemannian Geometry, tensor calculus can be used to model space-time, represented by a 4-dimensional manifold. Thus, equations arise in mathematical physics (e.g. Yamabe's), where local geometries are studied by comparing (isometric) manifolds and their curvature. Of eight feasible geometries given by the "geometrization conjecture", the curvature of the observable Universe, or the local geometry, is in all likelihood described by one of the three "primitive" geometries:

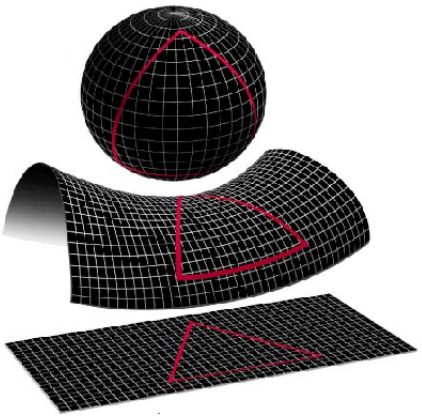

Figure 29: Three types of curvatures of the universe

A.5 The Laplace Operator

Recall how to define the Laplace operator. It is the sum of the second-order, partial derivatives, where is a domain in $\mathbb{R}^n$.

Dimension n: $\Delta = \sum_{i=1}^{n} \frac{\partial^2}{\partial x_i^2}$

$u: \quad \subset \mathbb{R}^n \to \mathbb{R},$

$x = (x_1, x_2, \ldots, x_n) \quad \Rightarrow \quad \Delta u(x) = \sum_{i=1}^{n} \frac{\partial^2 u(x)}{\partial x_i^2}$

Laplace Operator in Spherical Coordinates

$x = r\cos(\theta)\sin(\phi)$ $\qquad$ $r = \sqrt{x^2 + y^2 + z^2}$
$y = r\sin(\theta)\sin(\phi)$ $\qquad$ $\theta = \arctan(\frac{y}{x})$
$z = r\cos(\phi)$ $\qquad$ $\phi = \arccos(\frac{z}{r})$

$u: \quad \subset \mathbb{R}^3 \to \mathbb{R}$
$u(x, y, z) = v(r, \theta, \phi)$

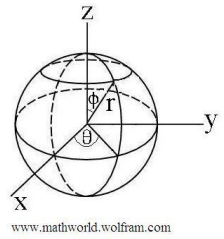

$$\Delta u \;=\; u_{xx} + u_{yy} + u_{zz} \;=\; \mathbf{v_{rr}} + \mathbf{\frac{2}{r}v_r} + \mathbf{\frac{1}{r^2}v_{\theta\theta}} + \mathbf{\frac{1}{r^2\sin^2\theta}v_{\phi\phi}} + \mathbf{\frac{\cos\theta}{r^2\sin\theta}v_\phi}$$

A.6 Linearization

Linearizing a nonlinear differential equation of the form

$$D[u] = g(u)$$

(D is the differential operator and g is a nonlinear function) means substituting g by its tangent line approximation, $L(u) = g(u_0) + g'(u_0)(u - u_0)$. This tangent line approximation is taken about a point u_0 satisfying $g(u_0) = 0$ and $g'(u_0) \neq 0$.

For example, if we use our PDE (5), then

$$\begin{aligned} D[u] &= -\Delta u \\ g(u) &= \lambda u + u^p \\ u_0 &\equiv 0 \end{aligned}$$

The tangent line approximation is

$$g(u_0) + (u - u_0)g'(u_0) = 0 + u(\lambda + (5)(0^4)) = \lambda u.$$

The linearized PDE becomes $-\Delta u = \lambda u$.

A.7 Radial Symmetry

A function $u : \quad \to \mathbb{R}$ is said to be radially symmetric or to have the radial symmetry property if it is independent of all angles (θ, ϕ, etc.) and depends exclusively on $r = \|x\|$, $x \in \quad \subset \mathbb{R}^n$. The following figure shows two functions defined over $\quad$ = unit ball in $\mathbb{R}^2$ that have the radial symmetry property.

A.8 Yamabe's Problem

An important problem in general relativity is to tell when two space-times represented by two Riemannian manifolds are 'locally the same,' or isometric. In the field of differential geometry, this question is addressed in a classical problem called the Yamabe Problem:

$$-\Delta_g u = u^{(n+2)/(n-2)} + [\frac{n-2}{4(1-n)} R_g]u, \quad u > 0, \quad M, \tag{18}$$

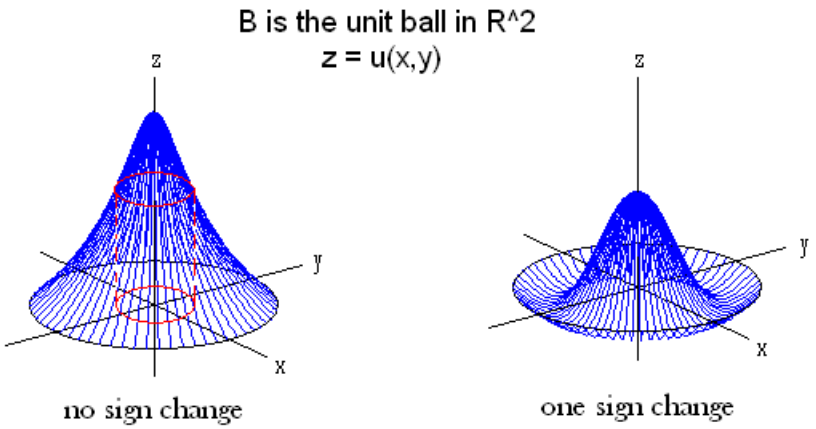

where M is any manifold. When solving (18), the hardest case turned out to be that of a sphere. There is a vast family of Yamabe-type problems, including those that accommodate the case of noncompact Riemannian manifolds or manifolds with a boundary (for instance [17, 16, 8, 7]).

B Acknowledgements

This research was conducted at the Applied Mathematical Sciences Summer Institute (AMSSI) and has been partially supported by grants given by the Department of Defense (through its ASSURE program), the National Science Foundation (DMS-0453602), and National Security Agency (MSPF-06IC-022). Substantial financial and moral support was also provided by Don Straney, Dean of the College of Science at California State Polytechnic University, Pomona. Additional financial and moral support was provided by the Department of Mathematics at Loyola Marymount University and the Department of Mathematics & Statistics at California State Polytechnic University, Pomona. This project would not have been possible without the help of Dr. Maria Mercedes Franco and Michelle Craddock; a special thanks to them and all the AMSSI faculty. The authors are solely responsible for the views and opinions expressed in this research; it does not necessarily reflect the ideas and/or opinions of the funding agencies and/or Loyola Marymount University or California State Polytechnic University, Pomona.

References

[1] F.V. Atkinson, H. Brezis, and L.A. Peletier. Solutions d'équations elliptiques avec exposant de sobolev critique qui changent de signe. *C.R. Acad. Sci. Paris*, 306:711–714, 1988.

[2] H. Brezis and L. Nirenberg. Positive solutions of nonlinear elliptic equations involving critical sobolev exponents. *Communications in Pure and Applied Mathematics*, 36, 1983.

[3] R. Burden and J. Faires. *Numerical Analysis*. Thomson, United States, eighth edition, 2005.

[4] G. Cerami, D. Fortunato, and M. Struwe. Bifurcation and multiplicity results for nonlinear elliptic problems involving critical sobolev exponents. *Ann Inst Henri Poincaré*, 1(5):341–350, 1984.

[5] G. Cerami, S. Solimini, and M. Struwe. Some existence results for superlinear elliptic boundary value problems involving critical exponents. *Journal of Functional Analysis*, 69, 1986.

[6] Y. Deng and Y. Li. Existence and bifurcation of the positive solutions for a semilinear equation with critical exponent. *Journal of Differential Equations*, 130:179–200, 1996.

[7] J. F. Escobar. Positive solutions for some semilinear elliptic equations with critical sobolev exponents. *Communications on Pure and Applied Mathematics*, 40, 1987.

[8] J. F. Escobar. The yamabe problem on manifolds with boundary. *Journal of Differential Geometry*, 35, 1992.

[9] D. Fortunato and E. Janelli. Infinitely many solutions for some nonlinear elliptic problems in symmetrical domains. *Proceedins of the Royal Society of Edinburgh*, 105, 1987.

[10] M. Franco. *Aproximacion Numerica de Soluciones Radiales para Problemas Semilineales Elipticos*. B.S. dissertation, Universidad del Valle, Departamento de Matematicas, 1999.

[11] H. Grunau G. Arioli, F. Gazzola and E. Sassone. The second bifurcation branch for radial solutions of the brezis-nirenberg problem in dimension four. *Scuola Normale Superiore and Dept. of Math - Calculus of Variations and Geometric Measure Theory*, 2006.

[12] B. Gidas, W. M. Ni, and L. Nirenberg. Symmetry and related properties via the maximum principle. *Comm. Math. Phys.*, 68, 1979.

[13] J. Dolbeault M. del Pino and M. Musso. Duality in sub-supercritical bubbling in the brezis-nirenberg problem near the critical exponent. *http://www.ceremade.dauphine.fr/ dolbeaul/Preprints/pasi2.pdf*. Preprint.

[14] The MathWorks. Accelerating the pace of engineering and science. *http://www.mathworks.com/products/mathlab*.

[15] S. I. Pohozaev. Eigenfunctions of the equation $\delta u + \lambda f(u) = 0$. *Soviet Math. Dokl*, 6, 1965.

[16] N. Trudinger. Remarks concerning the conformal deformation of riemannian structures on compact manifolds. *Ann. Sc. Norm. Sup. Pisa*, 22, 1968.

[17] H. Yamabe. On a deformation of riemannian structures on compact manifolds. *Osaka Math. J.*, 12, 1960.

[18] D. Zwillinger. *Handbook of Differential Equations*. Academic Press, United States, third edition, 1988.